NASA Technical Memorandum 103623

Solar Radiation on Mars—Update 1990

Joseph Appelbaum
Tel Aviv University
Tel Aviv, Israel

and

Dennis J. Flood
Lewis Research Center
Cleveland, Ohio

October 1990

NASA

SOLAR RADIATION ON MARS

UPDATE 1990

Joseph Appelbaum* and Dennis J. Flood
National Aeronautics and Space Administration
Lewis Research Center
Cleveland, Ohio 44135

SUMMARY

Detailed information on solar radiation characteristics on Mars are necessary for effective design of future planned solar energy systems operating on the surface of Mars. In this paper we present a procedure and solar radiation related data from which the diurnally and daily variation of the global, direct beam and diffuse insolation on Mars are calculated. The radiation data are based on measured optical depth of the Martian atmosphere derived from images taken of the sun with a special diode on the Viking Lander cameras; and computation based on multiple wavelength and multiple scattering of the solar radiation. This work is an update to NASA TM-102299 and includes a refinement of the solar radiation model.

INTRODUCTION

Missions to the Martian surface will require electric power. Of the several possibilities, photovoltaic power systems can offer many advantages, including high power to weight, modularity, scalability, and a long history of successful application in space. To design a photovoltaic system, detailed information on solar radiation data on the Martian surface is necessary to allow more accurate estimates of photovoltaic power system size and mass in system analysis and trade-off studies of relevant technology options.

This report is an update to NASA TM-102299 (ref. 1) and to the paper (ref. 2) on "Solar Radiation on Mars." We present a procedure and solar radiation data from which the diurnally and daily variation of the global, direct beam and diffuse insolation are calculated. The calculation of these quantities became possible with the introduction of the "normalized net solar flux function" based on multiple wavelength and multiple scattering of the solar radiation. The solar radiation data presented in this report pertain again to the two Viking Lander locations VL1 (22.3° N, 47.9° W) and VL2 (47.7° N, 225.7° W). This update report include a refinement of the solar radiation model. The opacities at the two Viking Landers were updated, the net solar flux function was extended for albedo 0.4, and an analytical expression for the net solar flux function was formulated. In addition, the solar radiation calculations were extended to include the daylight hours and the daily insolation on a horizontal surface for a Martian year calculated for each 5° of areocentric longitudes.

*National Research Council - NASA Research Associate; present address Tel Aviv University, Tel Aviv, 69978 Israel. Work funded under NASA grant NAGW-2022.

OPTICAL DEPTH

The most direct and probably most reliable estimates of opacity are those derived from Viking Lander imaging of the Sun. Figures 1 and 2 show the seasonal variation of the normal-incidence of the optical depth at the Viking Lander locations VL1 and VL2, respectively. The season is indicated by the value of L_S areocentric longitude of the Sun, measured in the orbital plane of the planet from its vernal equinox, $L_S = 0°$. Figures 1 and 2 were derived from (ref. 3) and were discretized for each 5° (see measured and discretized). The optical depth is assumed to remain constant throughout the day. Opacities are minimum during the northern spring (L_S = 0° to 90°) and summer (L_S = 90° to 180°), and maximum during southern spring (L_S = 180° to 270°) and summer (L_S = 270° to 360°), the seasons during which most local and major dust storms occur. When dust storms are not present, the optical depth is typically about 0.5. Two global dust storms occurred during the periods of each observation as indicated by the high values of the optical depth (they are lower bound values). Figures 3 and 4 show the variation of the optical depth of figures 1 and 2 in greater detail.

DUST STORMS

Observation from Earth, from orbit around Mars, and from the surface of the planet itself have shown that airborne dust is a highly variable and thermodynamically significant component of the Martian atmosphere. Martian dust plays a key role in determining the current climate of Mars, and is suspected of having a major influence on the evolution of the surface and the history of climatic conditions on the planet. Airborne dust may be transported over short or long distance depending upon regional meteorological conditions. Dust is raised from the surface into the atmosphere, and when certain conditions are met, it may be translated into local or global dust storms. The spacial distribution of dust storms and of changes in surface albedo suggest that dust can be removed from the surface almost anywhere on the planet. There may be long periods when little dust moves at all at some locations, while there appear to be other regions where dust is raised more frequently. Many of the parameters controlling the location, severity, and frequency of dust-raising activity are not well understood. The classical view is that dust storm activity is correlated with a general intensification of winds around the time of maximum insolation, near southern summer solstice and perihelion. Dust storms are distinguished as minor or major storms, the former being localized clouds that remain locally and dissipate in a few days or so. Major dust storms are also called "global" or "great" storms and are classified as regional or planet-encircling storms. Local storms appear to play an important role in initiating the global storms. The thermodynamics of local storm generation and the mechanisms by which local storms become planet-recircling storms remain obscure. During the planet-encircling dust storms, dust is raised and spread over much of the planet for many Martian days (sols), and eventually falls to the surface. The direction of the dust transport of these storms is that dust is moved about within the southern hemisphere or from the south to the north over several weeks. The atmospheric dust decreases the amount of insolation reaching the surface, increases the infrared atmosphere heat flux, and absorb radiation emitted by the surface. The intensity of the dust storms are defined in terms of the optical depth of the Martian atmosphere. From a photovoltaic system design point of view, the intensity, frequency, and duration of these

storms may be viewed as "partially cloudy" and "cloudy" days for which additional energy storage must be taken into account. The characteristics of the global and local dust storms are discussed in the following subsections.

Global Dust Storms

(Regional and Planet-Encircling Dust Storms)

The regional and planet-encircling dust storms are defined as:

Regional: regional in area, with the long axis of the affected area >2000 km, but did not encircle the planet.

Planet-encircling: area affected encircled the planet, usually in the east-west direction. Storm cover much of one or both hemisphere

Their characteristics are:

- One or more dust storms of regional or larger size can occur in any given Mars year. When they do occur, there is significant variation in their duration, areal extent and general opacity.

- There are many Mars years in which no planet-encircling dust storm has occurred; less frequently, there may be years in which not even regional storms occur.

- The relatively rare planet-encircling storms may have occurred more frequently during the last two decades (the period of spacecraft exploration of Mars!) than earlier in the century; these storms all occurred within 90° L_S of perihelion.

- The duration of these dust storms may vary from 35 to 70 days or more.

- The storms begin near perihelion, when solar radiation is maximum (southern spring and summer) in the southern mid-latitude.

- The first global dust storm observed by the Viking Landers (1977) spread from a latitude of 40° S to a latitude 48° N in about 5 to 6 days.

- The opacity of the atmosphere during the global dust storms is greater than 1.

Local Dust Storms

- Local dust storms occur at almost all latitudes and throughout the year. However, they have observed to occur most frequently in the approximate latitude belt 10° to 20° N and 20° to 40° S, with more dust clouds seen in the south than in the north, the majority of which occurred during southern spring.

- Based on Viking orbiter observations, it is estimated that approximately 100 local storms occur in a given Martian year.

- Local dust storms last a few days.

SURFACE ALBEDO

The albedo of a surface is a measure of the incident solar radiation reflected by the surface. The albedo behavior of Mars was measured by the Viking infrared thermal mapper (IRTM) instruments in the range of 0.3 to 3.0 μm (ref. 4). Global dust storms on Mars plays an important role in the deposition and removal of fine dust materials. The major variation in albedo were associated with the two global dust storms of 1977. During the seasons that are free of global dust storms, the observed albedo was reasonably uniform. Between the two storms, the atmosphere cleared substantially with many southern hemisphere regions returning to their prestorm albedos. The northern hemisphere atmosphere retained dust longer during the decay phase of the storms than the southern hemisphere. Southern hemisphere dark regions were not measurably brighter following the global storm suggesting little net deposition of dust (rate less than 0.15 ~ 1.5 μm/year). In contrast, the northern hemisphere dark regions of Syrtis Major and Acidalia Planitia were measurably brighter following the storms, indicating a deposition of dust. These surfaces subsequently darkened over the following months returning to prestorm albedo values. Dust is also deposited in bright, low-inertia regions (at a rate a few to ~45 μm/year), where it remains. Remote sensing observations indicate that major dust deposits are currently located in three northern equatorial regions: Tharsis, Arabia and Elysium. They are covered by fine (~2 to 40 μm) bright (albedo >0.27) particles.

Considering solar collectors operation on the Martian surface in the context of dust deposition on the collectors and the change in the nearby surface albedo, we may take into account the following: the amount of solar radiation at perihelion and maximum wind velocities occur in the south causing storm initiation, whereas regional dust deposition occur in the north suggesting net transport of dust from south to north. In the south, very small amounts of dust are deposited, whereas in the north there are regional dust deposits remaining on the surface for a length of time (few months), and there are regions where the dust accumulate and remain.

SOLAR RADIATION AT THE TOP OF MARS ATMOSPHERE

The variation of the solar radiation at the top of the Mars atmosphere is governed by the location of Mars in its orbit and by the solar zenith angle. The solar radiation is direct beam radiation. The beam irradiance, in W/m^2, is given by:

$$G_{ob} = \frac{S}{r^2} \tag{1}$$

where S is the solar constant at the mean Sun-Earth distance of 1 AU, i.e., $S = 1371\ W/m^2$; r is the instantaneous Sun-Mars distance in AU (heliocentric distance) given by (ref. 5):

$$r = \frac{a(1 - e^2)}{1 + e \cos \theta} \tag{2}$$

where a is the Mars semi-major axis in AU, and e is the Mars eccentricity, i.e., $e = 0.093377$; and θ is the true anomaly given by:

$$\theta = L_s - 248° \tag{3}$$

where L_s is the areocentric longitude and 248° is the areocentric longitude of Mars perihelion. The Sun-Mars mean distance in astronomical units (AU) is 1.5236915; therefore, the mean beam irradiance at the top of the Martian atmosphere is: $1371/1.5236915^2 = 590$ W/m^2. The instantaneous beam irradiance is given by equations (1) to (3).

$$G_{ob} = 590 \frac{\left[1 + e \cos(L_s - 248)\right]^2}{(1 - e^2)^2} \tag{4}$$

and is shown in figure 5.

SOLAR RADIATION ON THE SURFACE OF MARS

The variation of the solar radiation on the Martian surface is governed by three factors: (1) the Mars-Sun distance, (2) solar zenith angle, and (3) the opacity of the Martian atmosphere. The global solar irradiance G is the sum of the direct beam irradiance G_b, the diffuse irradiance G_d, and the albedo G_{al}:

$$G = G_b + G_d + G_{al} \tag{5}$$

The direct beam irradiance on the Martian surface normal to the solar rays is related by Beer's law to the optical depth, τ, of the intervening atmospheric haze:

$$G_b = G_{ob} \exp[-\tau m(z)] \tag{6}$$

where $m(z)$ is the air mass determined by the zenith angle z, and can be approximated, for zenith angles up to about 80°, by:

$$m(z) \cong \frac{1}{\cos z} \tag{7}$$

The zenith angle of the incident solar radiation is given by:

$$\cos z = \sin \phi \sin \delta + \cos \phi \cos \delta \cos \omega \tag{8}$$

where

ϕ latitude
δ declination angle
ω hour angle measured from the true noon westward

The solar declination angle is given by:

$$\sin \delta = \sin \delta_0 \sin L_s \tag{9}$$

where $\delta_0 = 24.936°$ is the Mars obliquity of rotation axis. The variation of the solar declination angle is shown in figure 6. The four seasons pertain here to the northern hemisphere, the reverse is true in the southern hemisphere. The ratio of Mars to Earth length of day is 24.65/24. It is convenient, for calculation purposes, to define a Mars hour, H, by dividing the Martian day (sol) into 24 hr. Using the same relationship between the Mars solar time T and the hour angle as for the Earth, we write:

$$\omega = 15T - 180 \tag{10}$$

This is shwon in figure 7. The final solar radiation results can then be adjusted by the above ratio to correspond to actual (terrestrial) time. The sunset hour angle is given by (ref. 6):

$$\omega_{ss} = \cos^{-1}(-\tan \phi \tan \delta) \tag{11}$$

$$\text{if} \quad |\phi| < \pi/2 - |\delta| \tag{12}$$

polar night: the Sun will neither rise nor set for the day

$$\text{for} \quad \phi < -\pi/2 + \delta \quad \text{or} \quad \phi > \pi/2 + \delta \tag{13}$$

polar day: the Sun will remain above the horizon all the day

$$\text{for} \quad \phi > \pi/2 - \delta \quad \text{or} \quad \phi < \pi/2 - \delta \tag{14}$$

The number of Mars daylight hours is given by:

$$T_d = \frac{2}{15} \cos^{-1}(-\tan \phi \tan \delta) \tag{15}$$

The solar irradiance on a horizontal Martian surface ($G_{al} = 0$) is given by:

$$G_h = G_{bh} + G_{dh} \tag{16}$$

where:

G_h global irradiance on a horizontal surface
G_{bh} direct beam irradiance on a horizontal surface
G_{dh} diffuse irradiance on a horizontal surface

The diffuse irradiance of the Martian atmosphere may be a result of a different mechanism than that for the Earth atmosphere, nevertheless, to a first approximation, we will apply equation (16) as for Earth-terrestrial calculations.

The global irradiance G_h on a horizontal surface is given by:

$$G_h = G_{ob} \cos z \frac{f(z,\tau,al)}{(1 - al)} \tag{17}$$

where "al" is the albedo, and $f(z,\tau,al)$ is called the normalized net flux function. The net solar flux integrated over the solar spectrum on the Martian surface was calculated by Pollack (ref. 7) based on multiple wavelength and multiple scattering of the solar radiation. Derived data from this calculation are shown in tables I(a) and (b) for albedo = 0.1; and tables II(a) and (b) for albedo = 0.4. The parameters are the zenith angle z and the optical depth τ. For albedos between 0.1 and 0.4 a linear interpolation can be used. Figures 8 and 9 describe the variation of the normalized net flux function with optical depth and Sun zenith angle for 0.1 and 0.4 albedo, respectively, for some data in tables I and II. The normalized net flux function can be approximated by a polynomial expression given by:

$$f(z,\tau,al) = \left[\sum_{i=0}^{5}\sum_{j=0}^{5}\sum_{k=0}^{1} p(i,j,k) \cdot \tau^i \cdot \tilde{z}^j \cdot (al)^k\right](1 - al), \quad \tilde{z} = z/100 \tag{18}$$

where $p(i,j,k)$ are the coefficients of the polynomial given in table III. These coefficients were obtained from fitting equation (18) to the data in tables I and II based on the criteria of least square error. The mean error is about 0.7 percent for the full range. For zenith angles up to 40° the error is much smaller. The largest error is for zenith angle of 80° and 85° and for τ greater than 5. The maximum error is about 7 percent. At these large angles and opacities, the error has a minor effect on the calculated daily insolation.

Using equations (6) and (7), the beam irradiance G_{bh} on a horizontal surface is given by:

$$G_{bh} = G_{ob} \cos z \exp\left(\frac{-\tau}{\cos z}\right) \tag{19}$$

and the diffuse irradiance is obtained by subtracting the beam from the global irradiances (eqs. (17) and (19)). Figures 10 to 12 describe the variation of the global, beam and diffuse irradiances, respectively, on a horizontal Martian surface; and are given in pairs as functions of the optical depth τ and zenith angle z. The irradiances were calculated based on table I data and the mean irradiance of 590 W/m^2. The variation of the global irradiance G_h, equation (17) is shown in figures 10(a) and (b). The beam irradiance G_{bh} is obtained using equation (19) and is shown in figures 11(a) and (b). The beam irradiance shows a sharp decrease with increasing of the optical depth, and a relative moderate decrease with increasing of the zenith angle. The diffuse irradiance G_{dh} is shown in figures 12(a) and (b). The diffuse irradiance shows a sliding maximum with the variation of the zenith angle.

The actual (terrestrial) number of daylight hours, hr, is obtained by multiplying equation (15) by the ratio 24.65/24. These are given in table IV for different latitudes ϕ and areocentric longitudes L_s, and are also shown in figures 13(a) and (b).

The solar radiation (global, beam and diffuse) variation (diurnally and daily) can be calculated based on the preceding equations and the $f(z,\tau,al)$ table data. For a given L_s and ϕ, one can calculate the variation of the zenith angle z as function of the Mars solar time T using equations (8) to (10). Referring to figures 3 and 4 for the given L_s, the optical depth τ is determined. With tables I and II and equations (16), (17) and (19) one can calculate the solar radiation variation for the given day. The diurnal variation of the solar irradiances for $L_s = 141°$ and $L_s = 295°$ for albedo = 0.1 and for Viking Lander location VL1 are shown in figures 14(a) and (b), respectively. Areocentric longitude $L_s = 141°$ corresponds to the lowest opacity of 0.35, and $L_s = 291°$ to the highest opacity of 3.6 (fig. 3). The figures show clearly that at high opacity, the diffuse component dominates the solar radiation. The daily global insolation H_h, beam isolation H_b and diffuse isolation H_d can be calculated by integrating the irradiances over the period from sunrise to sunset. Table V gives the daily isolation (global, beam and diffuse) on a horizontal surface, in Whr/m^2-day at VL1 and VL2 for albedo = 0.1 for 72 areocentric longitudes covering a Martian year. The variation of the daily global isolation of table V is shown in figure 15.

CONCLUSIONS

Effective design and utilization of solar energy depend to a large extent on adequate knowledge of solar radiation characteristics in the region of solar energy system operation. In this paper we presented a procedure and solar radiation related data from which the diurnally and daily variation of insolation on Mars were calculated. This includes the global, beam and diffuse insolation on a horizontal surface, from which any desired solar radiation quantity can be derived for an engineering design. The global insolation on the surface of Mars was derived based on the normalized net solar flux function $f(z,\tau,al)$; the beam insolation was determined by Beer's law relating the isolation to the optical depth of the Martian atmosphere; and the diffuse insolation was calculated as the difference between the global and the beam insolation. The optical depths were measured at the two Viking lander locations, but can also be used, to the first approximation, for other locations.

Of major concern are the dust storms, which have been observed to occur on local as well as on global scales, and their effect on solar array output. In general, the assumption has been that global storms would reduce solar array output essentially to zero, because the opacity of the atmosphere may rise to values ranging from 3 to 9, depending on the severity of the storm. The two global dust storms that were observed in 1977 and the opacities measured by the two Viking Lander cameras, as seen in figures 3 and 4, may be considered as one of the worst years of dust activities on Mars. Even though, the opacities are relatively low during the northern spring and summer for more than a half Martian year or more than a terrestrial year (ref. 1) for which the insolation is relatively high varying from about 2 to 4 kWhr/m^2-day. It should also be noted

that there are many Mars years in which no planet-encircling dust storm has occurred; less frequently, there may be years in which not even regional storms occur. One of the most important results of this study is that there is a large diffuse component of the solar insolation, even at high opacity, so that solar energy system operation is still possible.

This report is an update to report NASA TM-102299 and includes a refinement of the solar radiation model. In particularly, the refinement pertains to the extension of the net solar flux function to albedo 0.4; the extension of this function to intermediate values of opacities; and the possibility of using the net solar flux function of albedo varying from 0.1 to 0.4.

ACKNOWLEDGMENT

This work was funded by NASA grant NAGW-2022. We are very grateful to James B. Pollack from the Space Science Division, NASA Ames Research Center for supplying use with the data from which the $f(z,\tau,al)$ tables were derived.

We thank the Department of the Interior - U.S. Geological Survey for supplying us with Mars Map, figure 16.

REFERENCES

1. Appelbaum, J.; and Flood, D.J.: Solar Radiation on Mars. NASA TM-102299, 1989.

2. Appelbaum, J.; and Flood, D.J.: Solar Radiation on Mars. Sol. Energy, vol. 45, no. 6, Nov. 9, 1990, pp. 353-363.

3. Colburn, D.S.; Pollack, J.B.; and Haberle, R.M.: Diurnal Variation in Optical Depth at Mars. ICARUS, vol. 79, May 1989, pp. 159-189.

4. Christensen, P.R.: Global Albedo Variation on Mars: Implications for Active Aelion Transport, Deposition, and Erosion. J. Geophys. Res., vol. 93, no. B7, July 10, 1988, pp. 7611-7624.

5. Smith, E.V.P.; and Jacob, K.C.: Introductory Astronomy and Astrophysics. W.B. Saunders Co., 1973.

6. Duffie, J.A.; and Beckman, W.A.: Solar Engineering of Thermal Processes. Wiley, 1980.

7. Pollack, J.B., et al.: Simulation of the General Circulation of Martian Atmosphere I: Polar Processes. J. Geophys. Res., vol. 95, no. B2, Feb. 1990, pp. 1447-1473.

TABLE I(a). - NORMALIZED NET FLUX FUNCTION $f(z,\tau,al)$ AT THE MARTIAN SURFACE.

ALBEDO 0.1									
Optical depth, τ	ZENITH ANGLE Z (DEG)								
	0.	5.	10.	15.	20.	25.	30.	35.	40.
.10	.883	.883	.883	.882	.881	.880	.879	.877	.875
.15	.875	.875	.874	.873	.872	.870	.868	.866	.862
.20	.866	.866	.865	.864	.862	.860	.857	.854	.850
.25	.857	.857	.856	.854	.852	.849	.846	.842	.838
.30	.848	.848	.847	.845	.842	.839	.835	.831	.826
.35	.839	.839	.838	.836	.833	.829	.824	.819	.813
.40	.830	.830	.829	.826	.823	.819	.814	.808	.801
.45	.822	.821	.820	.817	.814	.809	.804	.797	.790
.50	.813	.813	.811	.808	.804	.799	.793	.786	.778
.55	.805	.804	.802	.799	.795	.789	.783	.775	.767
.60	.796	.795	.793	.790	.785	.779	.772	.764	.755
.65	.787	.786	.784	.780	.775	.769	.762	.754	.743
.70	.778	.777	.775	.771	.766	.759	.752	.743	.732
.75	.770	.768	.766	.762	.757	.750	.742	.733	.721
.80	.761	.760	.757	.753	.748	.741	.732	.722	.711
.85	.752	.751	.748	.744	.739	.731	.722	.712	.701
.90	.744	.743	.740	.736	.730	.722	.713	.703	.690
.95	.736	.735	.732	.727	.721	.713	.703	.693	.680
1.00	.728	.727	.724	.719	.712	.704	.694	.683	.669
1.05	.720	.719	.716	.711	.704	.695	.685	.673	.659
1.10	.712	.711	.708	.703	.696	.687	.676	.664	.649
1.15	.704	.703	.700	.695	.688	.678	.667	.655	.640
1.20	.695	.694	.691	.686	.679	.669	.658	.645	.630
1.25	.687	.686	.683	.678	.670	.660	.649	.636	.621
1.30	.679	.678	.675	.670	.662	.652	.640	.627	.611
1.35	.672	.671	.668	.662	.654	.644	.632	.619	.602
1.40	.664	.663	.660	.654	.646	.636	.624	.611	.594
1.45	.657	.655	.652	.646	.638	.627	.615	.602	.585
1.50	.649	.648	.644	.638	.630	.619	.607	.593	.576
1.55	.642	.640	.637	.631	.622	.612	.599	.585	.568
1.60	.634	.633	.629	.623	.615	.604	.591	.577	.559
1.65	.627	.625	.621	.615	.607	.596	.583	.568	.551
1.70	.619	.618	.614	.608	.599	.588	.575	.560	.542
1.75	.612	.611	.607	.601	.592	.581	.568	.553	.534
1.80	.605	.604	.600	.594	.585	.574	.561	.546	.527
1.85	.598	.597	.593	.587	.578	.567	.553	.538	.520
1.90	.591	.590	.586	.580	.571	.559	.546	.531	.513
1.95	.584	.583	.579	.573	.564	.552	.539	.524	.506
2.00	.578	.576	.572	.566	.557	.546	.532	.517	.498
2.10	.564	.563	.558	.552	.543	.532	.518	.502	.483
2.20	.551	.549	.545	.539	.530	.518	.504	.489	.469
2.30	.538	.537	.533	.526	.517	.505	.492	.476	.457
2.40	.526	.524	.520	.514	.505	.493	.479	.464	.444
2.50	.514	.512	.508	.502	.493	.481	.467	.451	.432
2.60	.501	.499	.496	.489	.480	.468	.454	.438	.420
2.70	.489	.487	.483	.477	.468	.456	.441	.426	.407
2.80	.478	.477	.473	.466	.456	.445	.431	.415	.395
2.90	.467	.466	.462	.455	.446	.435	.421	.405	.385
3.00	.457	.456	.452	.445	.436	.425	.411	.395	.376
3.20	.436	.435	.431	.425	.416	.405	.391	.375	.357
3.40	.415	.414	.410	.404	.395	.384	.371	.356	.338
3.60	.395	.393	.389	.384	.376	.365	.352	.337	.319
3.80	.378	.376	.372	.367	.359	.349	.336	.321	.304
4.00	.363	.361	.357	.352	.344	.334	.321	.307	.290
4.50	.325	.323	.320	.315	.307	.297	.286	.272	.257
5.00	.289	.288	.285	.280	.273	.264	.253	.241	.227
5.50	.257	.256	.253	.249	.242	.234	.225	.213	.201
6.00	.229	.227	.224	.220	.215	.209	.200	.189	.178

TABLE I(b). - NORMALIZED NET FLUX FUNCTION $f(z,\tau,al)$ AT THE MARTIAN SURFACE.

ALBEDO 0.1									
Optical depth, τ	ZENITH ANGLE Z (DEG)								
	45.	50.	55.	60.	65.	70.	75.	80.	85.
.10	.872	.868	.862	.855	.844	.830	.804	.757	.640
.15	.858	.852	.844	.834	.819	.798	.762	.700	.566
.20	.844	.836	.826	.813	.794	.768	.724	.651	.508
.25	.831	.821	.808	.793	.770	.739	.688	.608	.466
.30	.818	.806	.791	.773	.747	.712	.656	.571	.433
.35	.804	.791	.774	.754	.726	.687	.627	.539	.407
.40	.790	.776	.758	.736	.706	.663	.599	.510	.385
.45	.778	.762	.742	.718	.686	.641	.575	.485	.367
.50	.765	.748	.727	.701	.667	.619	.551	.462	.351
.55	.753	.734	.712	.684	.648	.598	.528	.440	.337
.60	.741	.721	.697	.668	.631	.579	.508	.422	.325
.65	.728	.708	.683	.653	.615	.562	.491	.407	.315
.70	.716	.695	.669	.638	.600	.546	.474	.393	.306
.75	.705	.682	.655	.623	.585	.530	.457	.379	.297
.80	.693	.670	.642	.609	.570	.514	.442	.366	.288
.85	.682	.658	.630	.596	.556	.500	.429	.356	.281
.90	.671	.646	.617	.583	.543	.486	.416	.345	.274
.95	.660	.634	.605	.570	.528	.472	.403	.335	.267
1.00	.649	.623	.593	.557	.514	.459	.392	.324	.261
1.05	.638	.613	.582	.546	.503	.448	.382	.316	.255
1.10	.628	.602	.571	.535	.492	.438	.374	.309	.250
1.15	.618	.592	.561	.524	.480	.427	.364	.302	.245
1.20	.608	.581	.550	.513	.469	.416	.355	.295	.240
1.25	.598	.570	.539	.502	.457	.405	.346	.287	.235
1.30	.588	.560	.528	.491	.446	.395	.337	.280	.230
1.35	.579	.551	.519	.482	.437	.387	.331	.275	.226
1.40	.571	.542	.510	.473	.429	.379	.324	.270	.222
1.45	.562	.533	.501	.464	.420	.372	.318	.265	.219
1.50	.553	.524	.492	.455	.412	.364	.312	.260	.215
1.55	.544	.515	.483	.446	.403	.356	.305	.255	.211
1.60	.535	.506	.474	.437	.394	.348	.298	.249	.207
1.65	.527	.497	.465	.428	.385	.340	.292	.244	.203
1.70	.518	.489	.457	.420	.378	.333	.286	.240	.200
1.75	.511	.482	.450	.413	.371	.327	.281	.236	.197
1.80	.504	.475	.443	.406	.364	.321	.276	.232	.194
1.85	.496	.468	.436	.399	.358	.316	.272	.228	.191
1.90	.489	.460	.428	.392	.352	.310	.267	.225	.188
1.95	.482	.453	.421	.385	.345	.304	.262	.221	.185
2.00	.474	.445	.413	.377	.338	.298	.257	.217	.182
2.10	.459	.431	.399	.364	.325	.287	.248	.210	.176
2.20	.446	.417	.386	.352	.314	.276	.239	.203	.170
2.30	.433	.405	.374	.341	.304	.268	.232	.197	.166
2.40	.421	.393	.362	.330	.295	.260	.226	.192	.161
2.50	.409	.381	.351	.319	.285	.252	.219	.187	.157
2.60	.396	.369	.339	.308	.276	.243	.212	.181	.153
2.70	.384	.357	.328	.298	.266	.235	.205	.176	.148
2.80	.373	.347	.318	.289	.258	.228	.199	.171	.144
2.90	.363	.338	.310	.281	.251	.222	.193	.166	.140
3.00	.354	.329	.301	.273	.244	.216	.188	.162	.137
3.20	.336	.311	.285	.258	.231	.205	.179	.154	.131
3.40	.317	.294	.268	.243	.218	.193	.169	.146	.124
3.60	.299	.277	.253	.230	.206	.182	.160	.138	.117
3.80	.284	.263	.241	.218	.196	.174	.153	.132	.112
4.00	.271	.251	.229	.208	.187	.166	.146	.127	.107
4.50	.240	.222	.203	.184	.166	.148	.131	.114	.096
5.00	.212	.196	.179	.162	.146	.131	.116	.101	.086
5.50	.187	.173	.158	.143	.130	.116	.103	.090	.077
6.00	.166	.154	.141	.128	.116	.104	.093	.081	.069

TABLE II(a). - NORMALIZED NET FLUX FUNCTION $f(z,\tau,al)$ AT THE MARTIAN SURFACE.

ALBEDO 0.4									
Optical depth, τ	ZENITH ANGLE Z (DEG)								
	0.	5.	10.	15.	20.	25.	30.	35.	40.
.10	.596	.595	.594	.593	.592	.591	.590	.589	.588
.15	.592	.590	.590	.589	.588	.586	.585	.583	.582
.20	.587	.586	.585	.584	.583	.581	.579	.577	.575
.25	.583	.582	.581	.579	.578	.576	.574	.571	.569
.30	.578	.577	.576	.575	.573	.571	.568	.565	.562
.35	.574	.573	.572	.570	.568	.565	.563	.559	.556
.40	.569	.568	.567	.565	.563	.560	.557	.553	.549
.45	.565	.564	.563	.560	.558	.555	.552	.547	.542
.50	.560	.559	.558	.556	.553	.550	.546	.541	.535
.55	.555	.555	.553	.551	.548	.544	.540	.535	.529
.60	.550	.549	.548	.546	.543	.539	.534	.529	.522
.65	.545	.544	.543	.541	.538	.533	.528	.522	.516
.70	.540	.540	.538	.536	.532	.527	.522	.516	.509
.75	.535	.535	.533	.531	.527	.522	.516	.510	.503
.80	.531	.530	.528	.526	.522	.517	.511	.504	.496
.85	.526	.525	.523	.520	.517	.511	.505	.498	.490
.90	.521	.520	.518	.515	.511	.505	.499	.492	.483
.95	.516	.515	.514	.510	.506	.500	.494	.486	.476
1.00	.511	.511	.509	.506	.501	.495	.488	.480	.470
1.05	.506	.506	.504	.500	.496	.489	.482	.474	.464
1.10	.501	.501	.499	.495	.490	.483	.476	.468	.458
1.15	.497	.496	.494	.490	.485	.478	.471	.462	.452
1.20	.492	.491	.489	.485	.480	.473	.465	.456	.446
1.25	.487	.486	.484	.480	.475	.467	.460	.450	.439
1.30	.482	.481	.479	.475	.469	.462	.454	.445	.433
1.35	.477	.476	.474	.470	.464	.457	.449	.439	.428
1.40	.472	.471	.469	.465	.459	.452	.444	.434	.422
1.45	.467	.467	.465	.460	.455	.447	.438	.429	.417
1.50	.463	.462	.460	.456	.450	.442	.433	.423	.411
1.55	.458	.457	.455	.451	.445	.437	.428	.418	.406
1.60	.453	.452	.450	.446	.440	.432	.423	.413	.400
1.65	.449	.448	.445	.441	.435	.427	.418	.407	.395
1.70	.444	.443	.440	.436	.430	.422	.413	.402	.389
1.75	.440	.438	.435	.431	.425	.418	.408	.397	.384
1.80	.435	.434	.431	.427	.421	.413	.403	.392	.379
1.85	.431	.429	.427	.422	.416	.408	.398	.388	.375
1.90	.426	.425	.422	.417	.411	.403	.394	.383	.370
1.95	.422	.420	.418	.413	.406	.398	.389	.378	.365
2.00	.417	.416	.413	.408	.402	.394	.384	.373	.360
2.10	.408	.407	.404	.399	.393	.385	.375	.364	.350
2.20	.399	.398	.395	.391	.384	.376	.366	.355	.341
2.30	.391	.390	.387	.382	.376	.368	.358	.346	.332
2.40	.383	.382	.379	.374	.368	.359	.349	.338	.324
2.50	.375	.374	.371	.367	.360	.351	.341	.330	.316
2.60	.367	.365	.363	.358	.352	.343	.333	.321	.308
2.70	.358	.357	.354	.350	.343	.334	.324	.313	.299
2.80	.350	.349	.346	.342	.335	.326	.316	.305	.291
2.90	.343	.342	.339	.334	.328	.320	.310	.298	.284
3.00	.336	.335	.332	.327	.321	.313	.303	.291	.277
3.20	.322	.321	.318	.314	.307	.299	.289	.277	.264
3.40	.308	.307	.304	.300	.293	.285	.275	.264	.251
3.60	.294	.293	.290	.286	.280	.271	.262	.251	.238
3.80	.282	.281	.278	.274	.268	.260	.251	.239	.227
4.00	.271	.270	.267	.263	.257	.249	.240	.229	.217
4.50	.244	.243	.241	.237	.231	.224	.215	.205	.194
5.00	.219	.218	.216	.212	.207	.200	.192	.183	.173
5.50	.196	.196	.194	.190	.185	.179	.172	.163	.154
6.00	.176	.175	.173	.170	.166	.161	.154	.146	.137

TABLE II(b). - NORMALIZED NET FLUX FUNCTION $f(z,\tau,al)$ AT THE MARTIAN SURFACE.

ALBEDO 0.4									
Optical depth, τ	ZENITH ANGLE Z (DEG)								
	45.	50.	55.	60.	65.	70.	75.	80.	85.
.10	.586	.583	.579	.575	.568	.558	.540	.509	.430
.15	.579	.575	.569	.563	.553	.539	.514	.473	.382
.20	.571	.566	.559	.551	.538	.520	.490	.441	.344
.25	.564	.558	.549	.539	.524	.502	.467	.413	.316
.30	.557	.549	.539	.527	.509	.485	.447	.389	.295
.35	.549	.541	.529	.515	.496	.469	.428	.368	.278
.40	.542	.532	.519	.504	.483	.454	.411	.350	.264
.45	.534	.524	.510	.494	.471	.440	.394	.333	.252
.50	.526	.515	.501	.483	.459	.426	.379	.318	.242
.55	.519	.507	.491	.473	.448	.413	.365	.304	.233
.60	.512	.498	.482	.462	.437	.401	.352	.292	.225
.65	.505	.490	.473	.452	.427	.390	.340	.282	.219
.70	.498	.483	.465	.443	.417	.379	.329	.273	.213
.75	.491	.475	.456	.434	.407	.368	.318	.264	.207
.80	.483	.467	.448	.425	.397	.358	.308	.256	.202
.85	.476	.459	.440	.416	.389	.349	.300	.249	.198
.90	.470	.452	.432	.408	.380	.341	.292	.242	.193
.95	.463	.445	.424	.400	.371	.332	.283	.235	.189
1.00	.456	.438	.417	.392	.362	.323	.276	.228	.184
1.05	.450	.431	.410	.384	.354	.316	.270	.223	.180
1.10	.443	.424	.402	.377	.347	.309	.264	.219	.177
1.15	.437	.417	.396	.370	.339	.302	.258	.214	.174
1.20	.431	.411	.389	.363	.332	.295	.252	.209	.171
1.25	.424	.404	.382	.356	.324	.288	.246	.204	.167
1.30	.417	.398	.376	.349	.317	.281	.240	.200	.164
1.35	.412	.392	.370	.343	.311	.276	.236	.197	.162
1.40	.406	.386	.363	.337	.306	.271	.232	.193	.159
1.45	.400	.380	.357	.331	.300	.265	.227	.190	.157
1.50	.395	.374	.351	.325	.294	.260	.223	.186	.154
1.55	.389	.368	.346	.319	.288	.255	.219	.183	.152
1.60	.384	.363	.340	.313	.283	.250	.215	.180	.149
1.65	.378	.357	.334	.307	.277	.245	.211	.176	.147
1.70	.372	.352	.329	.302	.272	.240	.206	.173	.144
1.75	.367	.347	.324	.297	.267	.236	.203	.171	.142
1.80	.363	.342	.319	.292	.263	.232	.200	.168	.140
1.85	.358	.337	.314	.287	.258	.228	.197	.166	.138
1.90	.353	.332	.309	.283	.254	.224	.193	.163	.136
1.95	.348	.327	.304	.278	.250	.220	.190	.161	.134
2.00	.343	.322	.299	.273	.245	.217	.187	.158	.133
2.10	.333	.312	.289	.264	.237	.209	.181	.153	.129
2.20	.323	.303	.281	.256	.229	.202	.175	.149	.126
2.30	.315	.295	.273	.248	.222	.196	.170	.145	.122
2.40	.307	.287	.265	.241	.216	.191	.166	.142	.119
2.50	.299	.279	.257	.234	.209	.185	.161	.138	.116
2.60	.291	.271	.249	.227	.203	.179	.156	.134	.113
2.70	.283	.263	.242	.220	.197	.174	.151	.130	.110
2.80	.275	.255	.234	.213	.191	.169	.147	.127	.107
2.90	.268	.249	.228	.207	.186	.165	.144	.124	.104
3.00	.261	.243	.223	.202	.182	.161	.141	.121	.102
3.20	.249	.231	.211	.192	.172	.153	.134	.115	.097
3.40	.235	.218	.200	.181	.163	.145	.127	.110	.093
3.60	.223	.207	.189	.171	.154	.137	.121	.104	.089
3.80	.213	.197	.181	.164	.147	.131	.115	.100	.086
4.00	.204	.189	.173	.157	.141	.125	.110	.096	.082
4.50	.182	.168	.154	.140	.126	.112	.099	.087	.074
5.00	.161	.149	.136	.124	.113	.101	.090	.078	.066
5.50	.143	.133	.121	.110	.100	.091	.080	.070	.059
6.00	.128	.119	.109	.099	.090	.081	.072	.063	.054

TABLE III. - NORMALIZED NET FLUX FUNCTION COEFFICIENTS, $f(z,\tau,al)$

k = 0						
j \ i	0	1	2	3	4	5
0	1.002800	-.228681	.019613	.000231	-.000130	.000003
1	-.450073	1.335955	-1.131691	.402126	-.063967	.003758
2	5.566705	-16.912405	13.739701	-4.756079	.743740	-.043159
3	-22.471579	64.909973	-52.509470	17.997548	-2.786548	.160340
4	36.334497	-101.800319	79.895539	-26.762885	4.074117	-.231476
5	-20.420490	53.207148	-39.949537	12.977108	-1.931169	.107837
k = 1						
j \ i	0	1	2	3	4	5
0	.009814	.226139	-.117733	.030579	-.004090	.000218
1	-.156701	.396821	-.313648	.099227	-.013508	.000651
2	1.361122	-3.758111	3.007907	-.987457	.141693	-.007320
3	-4.365924	12.539251	-10.394165	3.486452	-.513123	.027401
4	5.991693	-17.498138	14.291370	-4.765323	.703675	-.037960
5	-2.915099	8.275686	-6.593125	2.173999	-.320308	.017335

TABLE IV. - DAYLIGHT HOURS (TERRESTRIAL), hr

Latitude, ϕ, DEG.									Ls
0	10	20	30	40	50	60	70	80	
12.32	12.32	12.32	12.32	12.32	12.32	12.32	12.32	12.32	0
12.32	12.38	12.43	12.49	12.57	12.67	12.83	13.12	13.97	5
12.32	12.43	12.53	12.66	12.81	13.01	13.33	13.92	15.69	10
12.32	12.48	12.64	12.82	13.05	13.35	13.83	14.73	17.60	15
12.32	12.53	12.74	12.99	13.29	13.69	14.33	15.56	19.96	20
12.32	12.58	12.84	13.15	13.52	14.03	14.83	16.41	24.65	25
12.32	12.62	12.94	13.30	13.75	14.36	15.33	17.30	24.65	30
12.32	12.67	13.04	13.46	13.98	14.69	15.83	18.24	24.65	35
12.32	12.71	13.13	13.61	14.20	15.01	16.32	19.26	24.65	40
12.32	12.76	13.22	13.75	14.41	15.32	16.81	20.42	24.65	45
12.32	12.80	13.30	13.88	14.60	15.61	17.29	21.86	24.65	50
12.32	12.83	13.38	14.00	14.79	15.89	17.75	24.65	24.65	55
12.32	12.87	13.45	14.12	14.96	16.14	18.18	24.65	24.65	60
12.32	12.90	13.51	14.22	15.11	16.37	18.59	24.65	24.65	65
12.32	12.92	13.56	14.30	15.23	16.56	18.95	24.65	24.65	70
12.32	12.94	13.60	14.37	15.33	16.72	19.25	24.65	24.65	75
12.32	12.96	13.63	14.42	15.41	16.84	19.48	24.65	24.65	80
12.32	12.97	13.65	14.45	15.45	16.91	19.62	24.65	24.65	85
12.32	12.97	13.66	14.46	15.47	16.93	19.67	24.65	24.65	90
12.32	12.97	13.65	14.45	15.45	16.91	19.62	24.65	24.65	95
12.32	12.96	13.63	14.42	15.41	16.84	19.48	24.65	24.65	100
12.32	12.94	13.60	14.37	15.33	16.72	19.25	24.65	24.65	105
12.32	12.92	13.56	14.30	15.23	16.56	18.95	24.65	24.65	110
12.32	12.90	13.51	14.22	15.11	16.37	18.59	24.65	24.65	115
12.32	12.87	13.45	14.12	14.96	16.14	18.18	24.65	24.65	120
12.32	12.83	13.38	14.00	14.79	15.89	17.75	24.65	24.65	125
12.32	12.80	13.30	13.88	14.60	15.61	17.29	21.86	24.65	130
12.32	12.76	13.22	13.75	14.41	15.32	16.81	20.42	24.65	135
12.32	12.71	13.13	13.61	14.20	15.01	16.32	19.26	24.65	140
12.32	12.67	13.04	13.46	13.98	14.69	15.83	18.24	24.65	145
12.32	12.62	12.94	13.30	13.75	14.36	15.33	17.30	24.65	150
12.32	12.58	12.84	13.15	13.52	14.03	14.83	16.41	24.65	155
12.32	12.53	12.74	12.99	13.29	13.69	14.33	15.56	19.96	160
12.32	12.48	12.64	12.82	13.05	13.35	13.83	14.73	17.60	165
12.32	12.43	12.53	12.66	12.81	13.01	13.33	13.92	15.69	170
12.32	12.38	12.43	12.49	12.57	12.67	12.83	13.12	13.97	175
12.32	12.32	12.32	12.32	12.32	12.32	12.32	12.32	12.32	180
12.32	12.27	12.22	12.16	12.08	11.98	11.82	11.53	10.68	185
12.32	12.22	12.12	11.99	11.84	11.64	11.32	10.73	8.96	190
12.32	12.17	12.01	11.83	11.60	11.30	10.82	9.92	7.05	195
12.32	12.12	11.91	11.66	11.36	10.96	10.32	9.09	4.69	200
12.32	12.07	11.81	11.50	11.13	10.62	9.82	8.24	0.00	205
12.32	12.03	11.71	11.35	10.90	10.29	9.32	7.35	0.00	210
12.32	11.98	11.61	11.19	10.67	9.96	8.82	6.41	0.00	215
12.32	11.94	11.52	11.04	10.45	9.64	8.33	5.39	0.00	220
12.32	11.89	11.43	10.90	10.24	9.33	7.84	4.23	0.00	225
12.32	11.85	11.35	10.77	10.05	9.04	7.36	2.79	0.00	230
12.32	11.82	11.27	10.65	9.86	8.76	6.90	0.00	0.00	235
12.32	11.78	11.20	10.53	9.69	8.51	6.47	0.00	0.00	240
12.32	11.75	11.14	10.43	9.54	8.28	6.06	0.00	0.00	245
12.32	11.73	11.09	10.35	9.42	8.09	5.70	0.00	0.00	250
12.32	11.71	11.05	10.28	9.32	7.93	5.40	0.00	0.00	255
12.32	11.69	11.02	10.23	9.24	7.81	5.17	0.00	0.00	260
12.32	11.68	11.00	10.20	9.20	7.74	5.03	0.00	0.00	265
12.32	11.68	10.99	10.19	9.18	7.72	4.98	0.00	0.00	270
12.32	11.68	11.00	10.20	9.20	7.74	5.03	0.00	0.00	275
12.32	11.69	11.02	10.23	9.24	7.81	5.17	0.00	0.00	280
12.32	11.71	11.05	10.28	9.32	7.93	5.40	0.00	0.00	285
12.32	11.73	11.09	10.35	9.42	8.09	5.70	0.00	0.00	290
12.32	11.75	11.14	10.43	9.54	8.28	6.06	0.00	0.00	295
12.32	11.78	11.20	10.53	9.69	8.51	6.47	0.00	0.00	300
12.32	11.82	11.27	10.65	9.86	8.76	6.90	0.00	0.00	305
12.32	11.85	11.35	10.77	10.05	9.04	7.36	2.79	0.00	310
12.32	11.89	11.43	10.90	10.24	9.33	7.84	4.23	0.00	315
12.32	11.94	11.52	11.04	10.45	9.64	8.33	5.39	0.00	320
12.32	11.98	11.61	11.19	10.67	9.96	8.82	6.41	0.00	325
12.32	12.03	11.71	11.35	10.90	10.29	9.32	7.35	0.00	330
12.32	12.07	11.81	11.50	11.13	10.62	9.82	8.24	0.00	335
12.32	12.12	11.91	11.66	11.36	10.96	10.32	9.09	4.69	340
12.32	12.17	12.01	11.83	11.60	11.30	10.82	9.92	7.05	345
12.32	12.22	12.12	11.99	11.84	11.64	11.32	10.73	8.96	350
12.32	12.27	12.22	12.16	12.08	11.98	11.82	11.53	10.68	355

TABLE V. - DAILY INSOLATION ON A HORIZONTAL SURFACE • Whr/m^2-day

VL1			VL2			Ls
Hbh	Hdh	Hh	Hbh	Hdh	Hh	
1599.19	1636.66	3235.85	646.44	1366.36	2012.80	0
1175.18	1829.13	3004.31	1003.72	1313.69	2317.41	5
1452.33	1731.73	3184.06	1286.08	1264.76	2550.84	10
1788.25	1581.39	3369.64	915.05	1502.53	2417.58	15
1695.98	1641.46	3337.44	1244.84	1442.63	2687.47	20
1712.34	1643.30	3355.64	1131.94	1564.41	2696.35	25
1959.92	1519.16	3479.08	1292.28	1565.45	2857.73	30
1849.52	1586.63	3436.15	1831.20	1351.34	3182.54	35
2110.70	1445.85	3556.55	2053.60	1292.21	3345.81	40
1751.51	1649.75	3401.26	1973.32	1403.80	3377.12	45
1650.85	1706.08	3356.93	1239.39	1818.20	3057.59	50
1295.14	1871.24	3166.38	2096.70	1451.56	3548.26	55
1659.76	1713.43	3373.19	2150.92	1473.70	3624.62	60
1771.34	1664.09	3435.43	2199.93	1494.51	3694.44	65
1892.12	1608.90	3501.02	2409.39	1416.41	3825.80	70
2023.48	1547.08	3570.56	2449.48	1432.68	3882.16	75
2032.76	1554.87	3587.63	2154.31	1629.51	3783.82	80
2043.77	1563.78	3607.55	2505.26	1455.29	3960.55	85
1812.62	1706.22	3518.84	2525.49	1466.16	3991.65	90
1715.04	1774.32	3489.36	2538.91	1474.84	4013.75	95
1728.60	1787.72	3516.32	2212.30	1673.38	3885.68	100
2243.87	1529.54	3773.41	2212.38	1684.39	3896.77	105
2263.49	1542.23	3805.72	2202.52	1685.70	3888.22	110
2599.01	1363.67	3962.68	2709.67	1375.86	4085.53	115
2621.38	1375.47	3996.85	3113.77	1096.27	4210.04	120
2642.75	1387.34	4030.09	2851.03	1239.17	4090.20	125
2662.26	1399.10	4061.36	2804.24	1232.88	4037.12	130
2679.02	1410.56	4089.58	2968.84	1081.02	4049.86	135
2875.66	1305.02	4180.68	2482.68	1338.12	3820.80	140
2371.10	1630.56	4001.66	2606.58	1200.54	3807.12	145
1958.75	1867.02	3825.77	2337.39	1307.72	3645.11	150
1953.33	1874.57	3827.90	2243.35	1288.70	3532.05	155
1822.25	1939.20	3761.45	2329.90	1151.06	3480.96	160
1805.09	1941.22	3746.31	1867.13	1338.66	3205.79	165
1670.50	1991.87	3662.37	1757.66	1306.78	3064.44	170
1641.60	1986.86	3628.46	972.12	1582.73	2554.85	175
1610.08	1991.49	3601.57	524.38	1604.87	2129.25	180
1055.67	2162.85	3218.52	324.34	1503.63	1827.97	185
835.21	2173.37	3008.58	487.57	1431.94	1919.51	190
913.36	2124.48	3037.84	515.82	1338.23	1854.05	195
1000.00	2063.58	3063.58	362.79	1257.98	1620.77	200
278.97	1954.24	2233.21	85.85	1048.88	1134.73	205
114.93	1691.47	1806.40	25.11	843.00	868.11	210
157.26	1744.39	1901.65	28.81	809.25	838.06	215
164.98	1722.49	1887.47	23.70	739.15	762.85	220
173.87	1699.92	1873.79	22.11	684.84	706.95	225
213.94	1709.19	1923.13	83.61	745.44	829.05	230
229.59	1686.40	1915.99	27.31	612.73	640.04	235
248.87	1665.24	1914.11	13.03	527.30	540.33	240
295.53	1657.91	1953.44	41.38	568.09	609.47	245
356.65	1648.39	2005.04	24.01	505.49	529.50	250
437.60	1634.12	2071.72	7.04	420.64	427.68	255
423.73	1608.84	2032.57	8.45	417.06	425.51	260
250.87	1539.96	1790.83	15.67	437.45	453.12	265
139.08	1431.42	1570.50	2.49	355.30	357.79	270
44.89	1205.98	1250.87	0.89	325.24	326.13	275
24.33	1088.60	1112.93	0.50	314.51	315.01	280
40.81	1188.80	1229.61	0.88	336.35	337.23	285
9.23	925.69	934.92	0.84	346.25	347.09	290
18.57	1049.20	1067.77	0.64	350.81	351.45	295
27.61	1131.48	1159.09	1.28	391.88	393.16	300
55.15	1284.71	1339.86	3.40	454.83	458.23	305
126.11	1480.25	1606.36	8.53	531.71	540.24	310
283.80	1657.91	1941.71	74.10	726.94	801.04	315
405.84	1728.95	2134.79	200.10	842.29	1042.39	320
463.43	1767.11	2230.54	189.27	899.60	1088.87	325
565.04	1802.06	2367.10	227.97	963.33	1191.30	330
683.86	1823.83	2507.69	218.84	1025.85	1244.69	335
625.66	1856.45	2482.11	86.00	995.97	1081.97	340
1123.67	1769.25	2892.92	336.17	1178.71	1514.88	345
949.68	1851.76	2801.44	425.65	1250.10	1675.75	350
1279.31	1761.39	3040.70	696.57	1273.39	1969.96	355

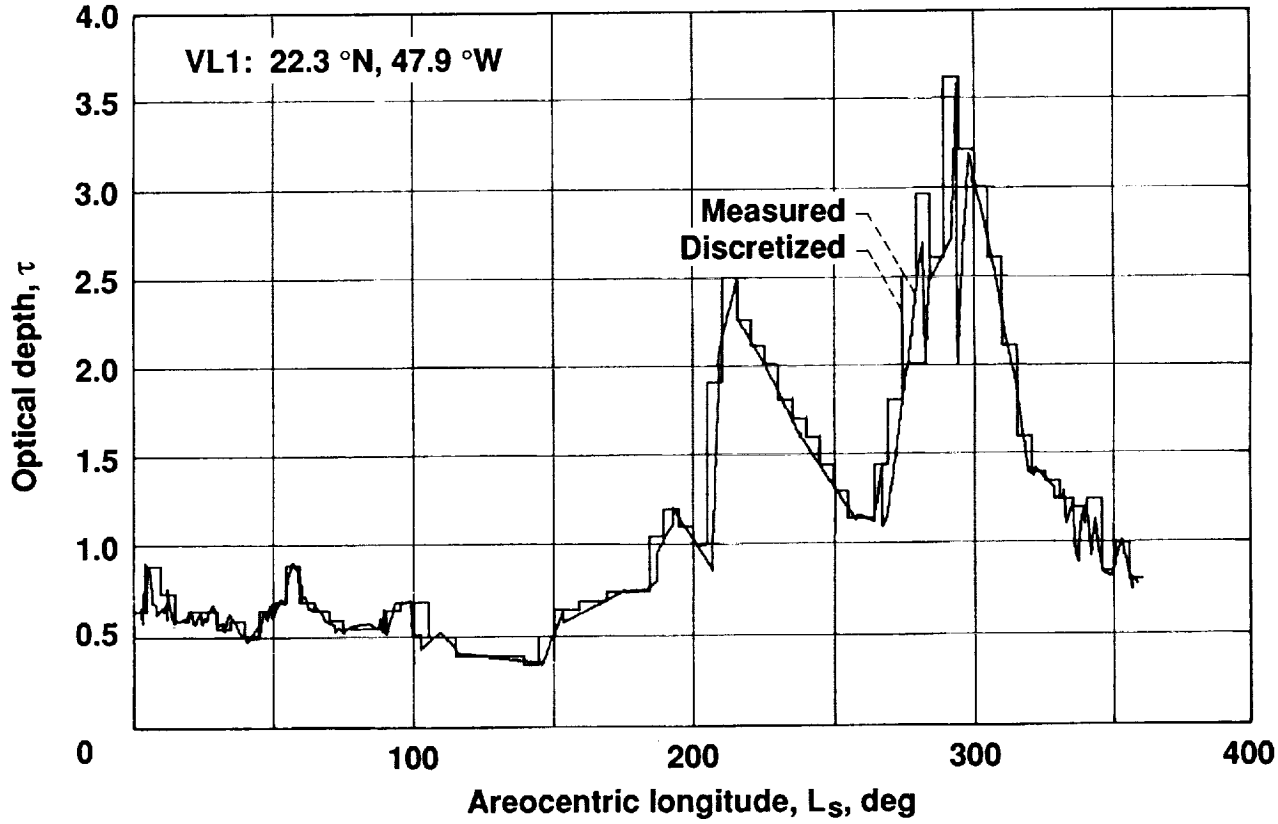

Fig. 1 - Measured and discretized optical depth at Viking Lander VL1

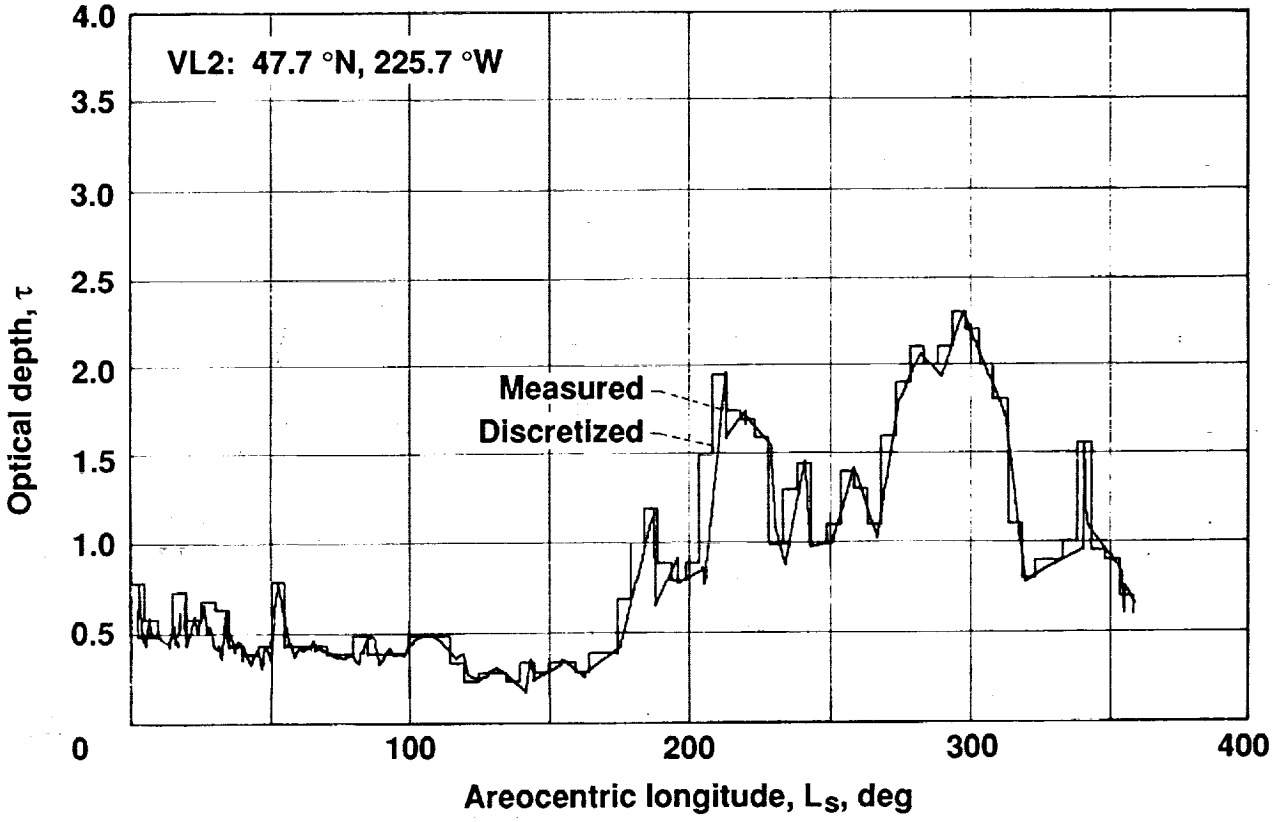

Fig. 2 - Measured and discretized optical depth at Viking Lander VL2

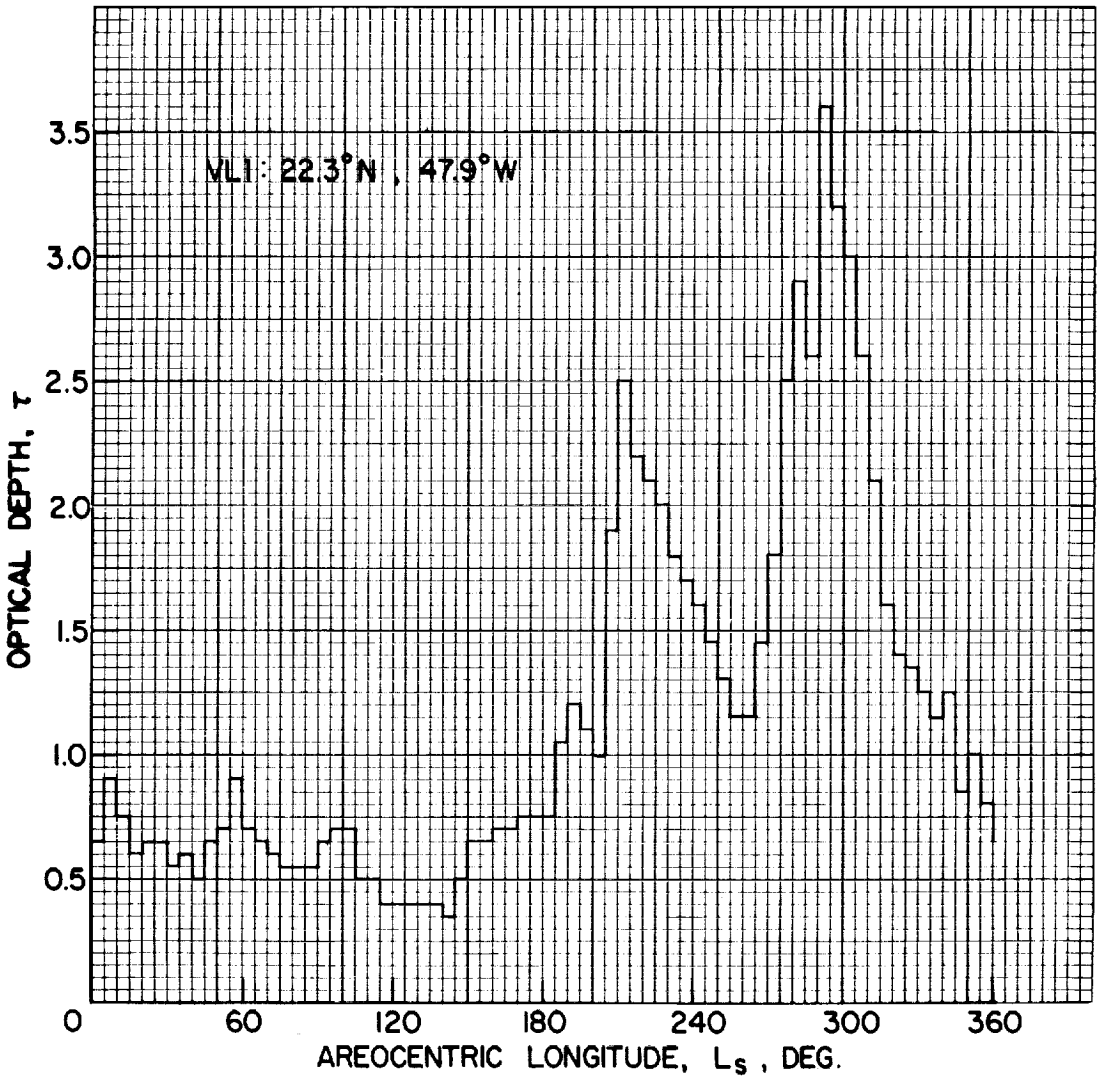

Fig. 3 - Optical depth at Viking Lander VL1 - in detail

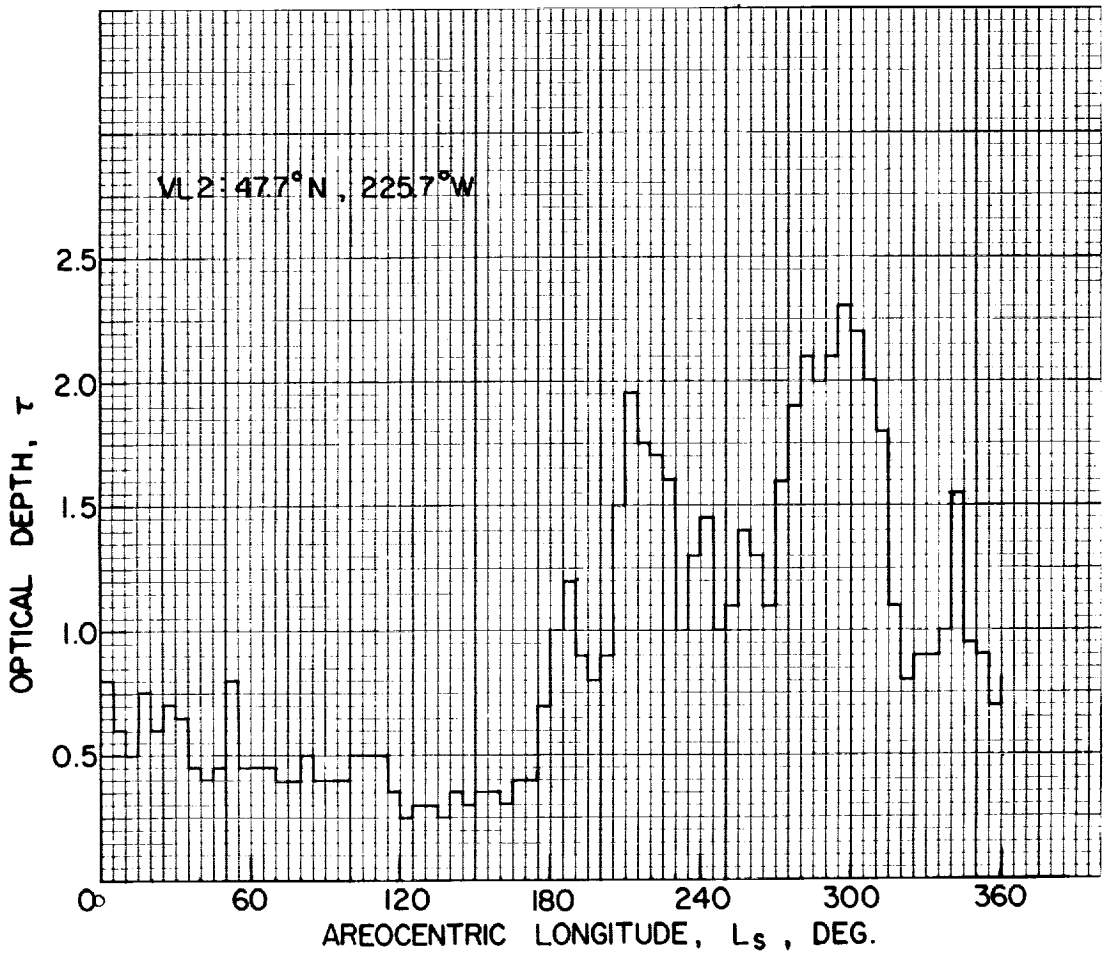

Fig. 4 - Optical depth at Viking Lander VL2 - in detail

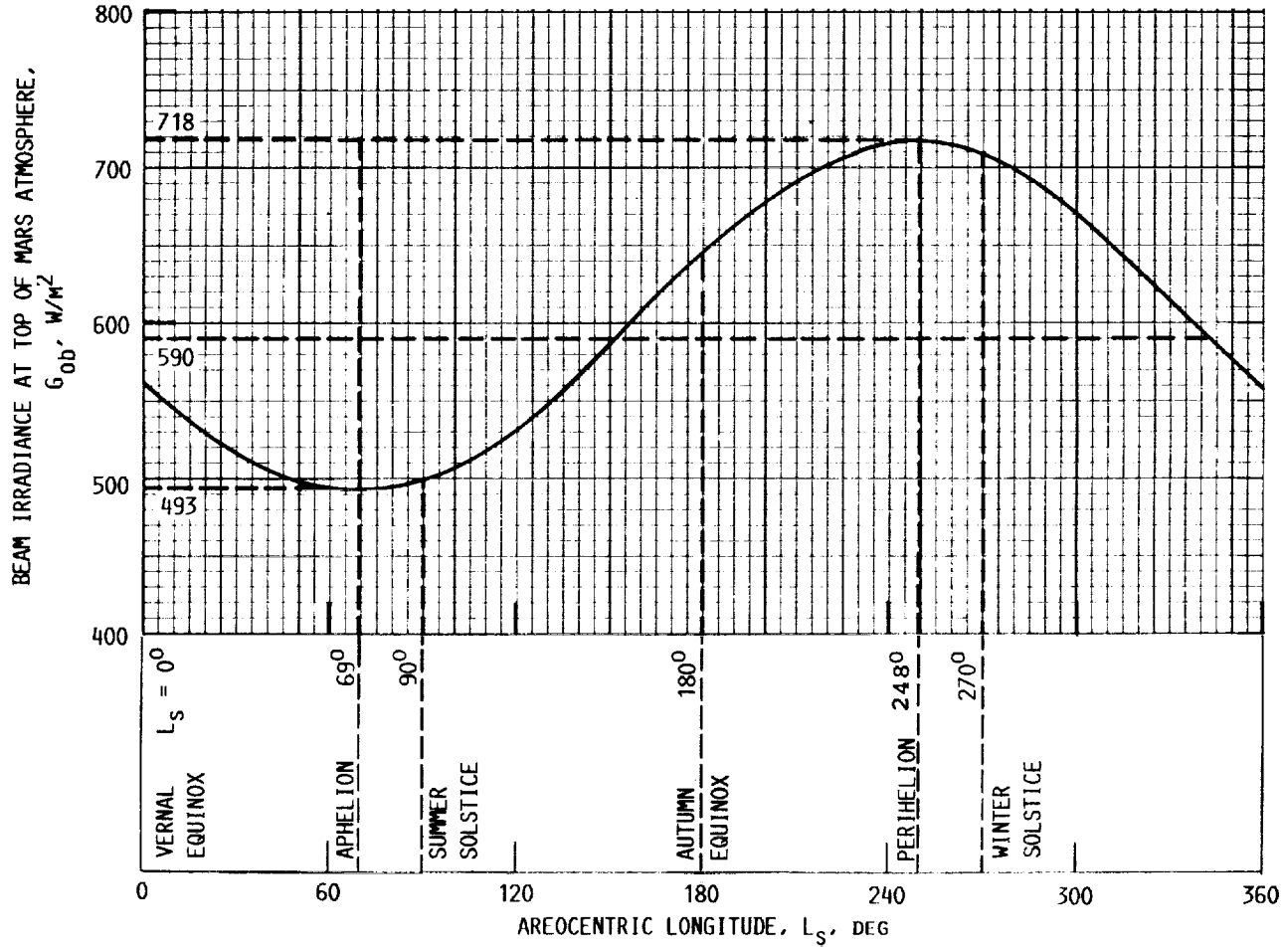

Fig. 5 - Beam irradiance at the top of Mars atmosphere as function of areocentric longitude

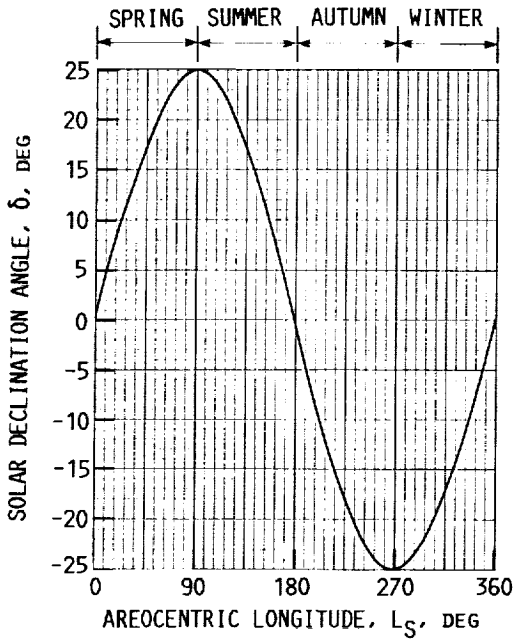

Fig. 6 - Variation of solar declination angle, δ, with areocentric longitude, L_S

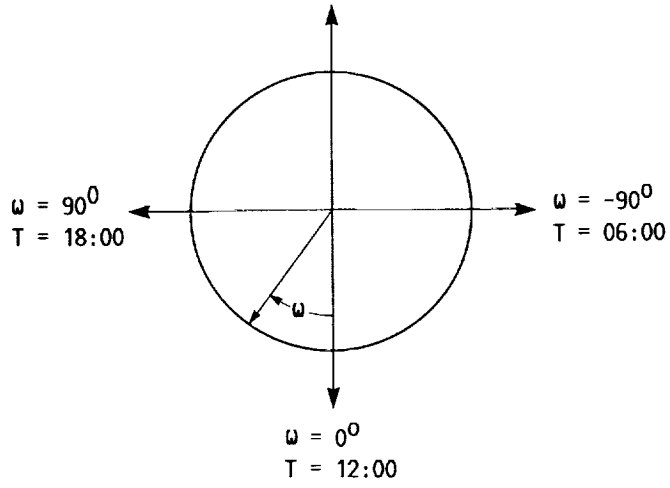

Fig. 7 - Solar time and hour angle relation

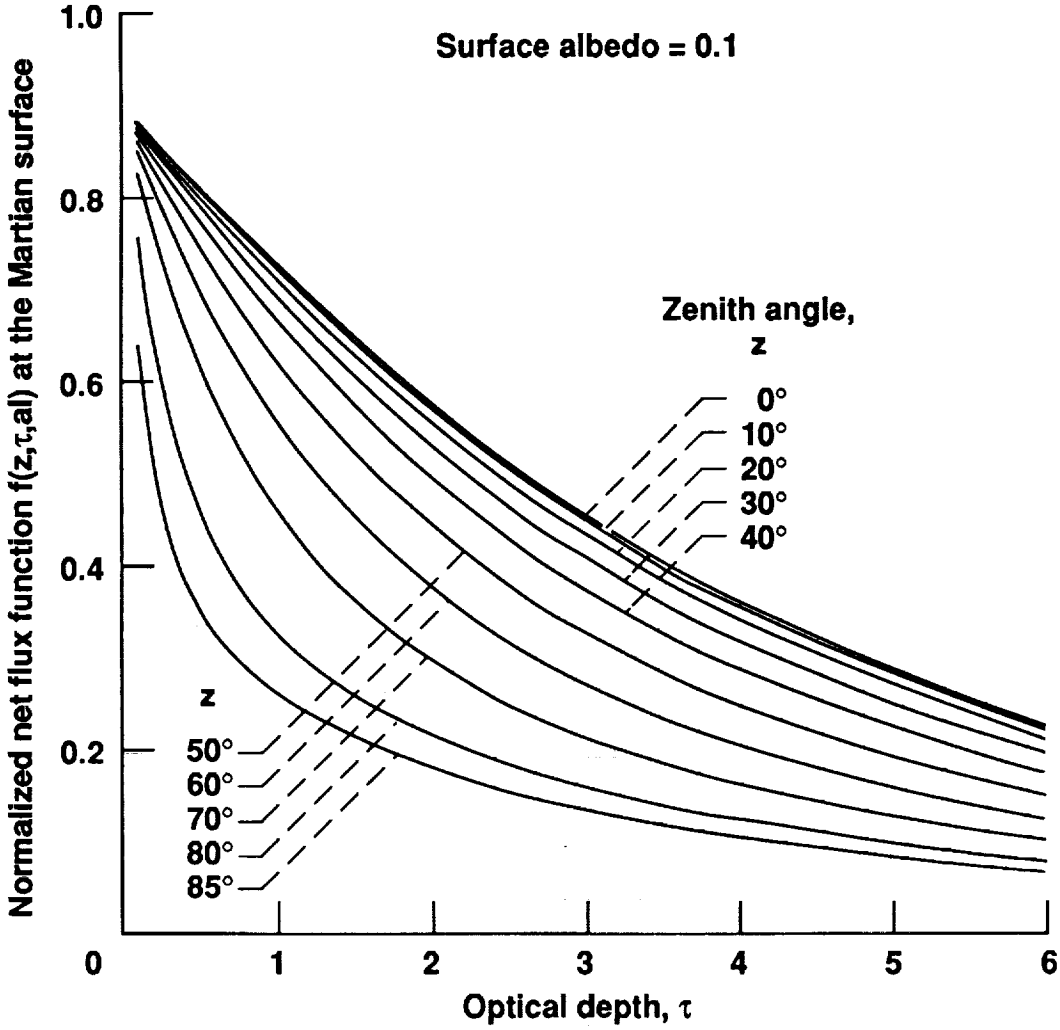

(a) Effect of optical depth with Sun zenith angle as a parameter

Fig. 8 - Variation of the normalized net flux function at the Martian surface with optical depth and Sun zenith angle, for albedo = 0.1

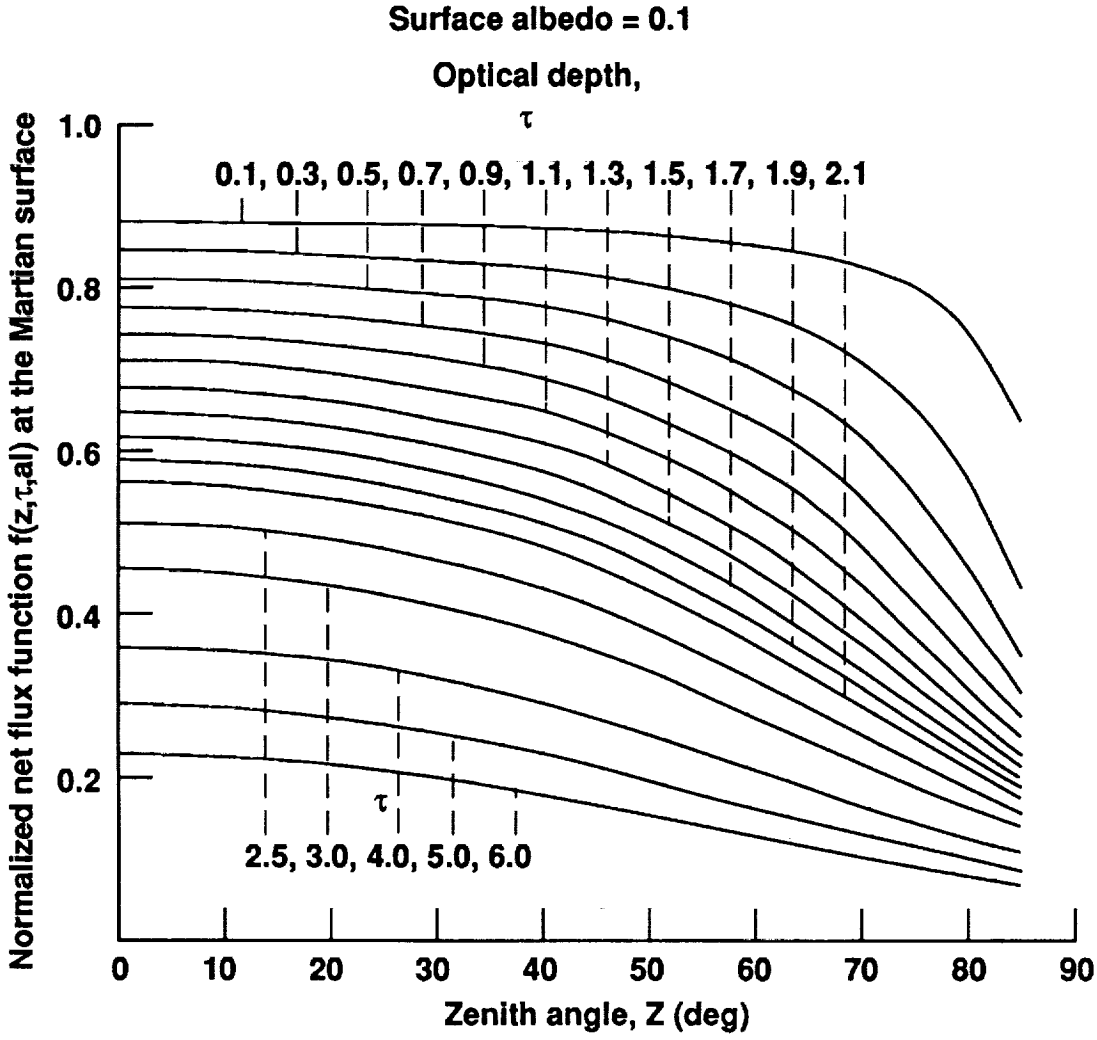

(b) Effect of Sun zenith angle with optical depth as a parameter

Fig. 8 - Concluded

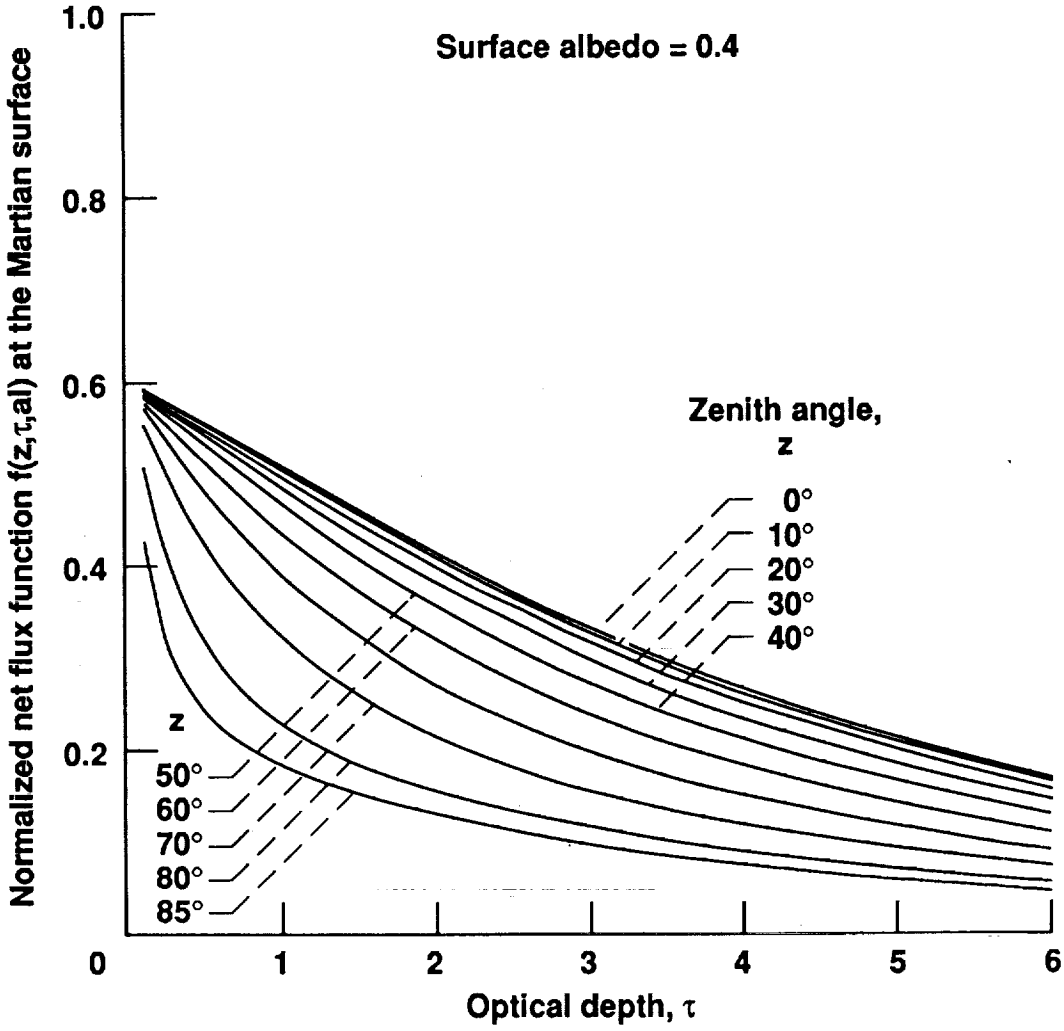

(a) Effect of optical depth with Sun zenith angle as a parameter

Fig. 9 - Variation of the normalized net flux function at the Martian surface with optical depth and Sun zenith angle, for albedo = 0.4

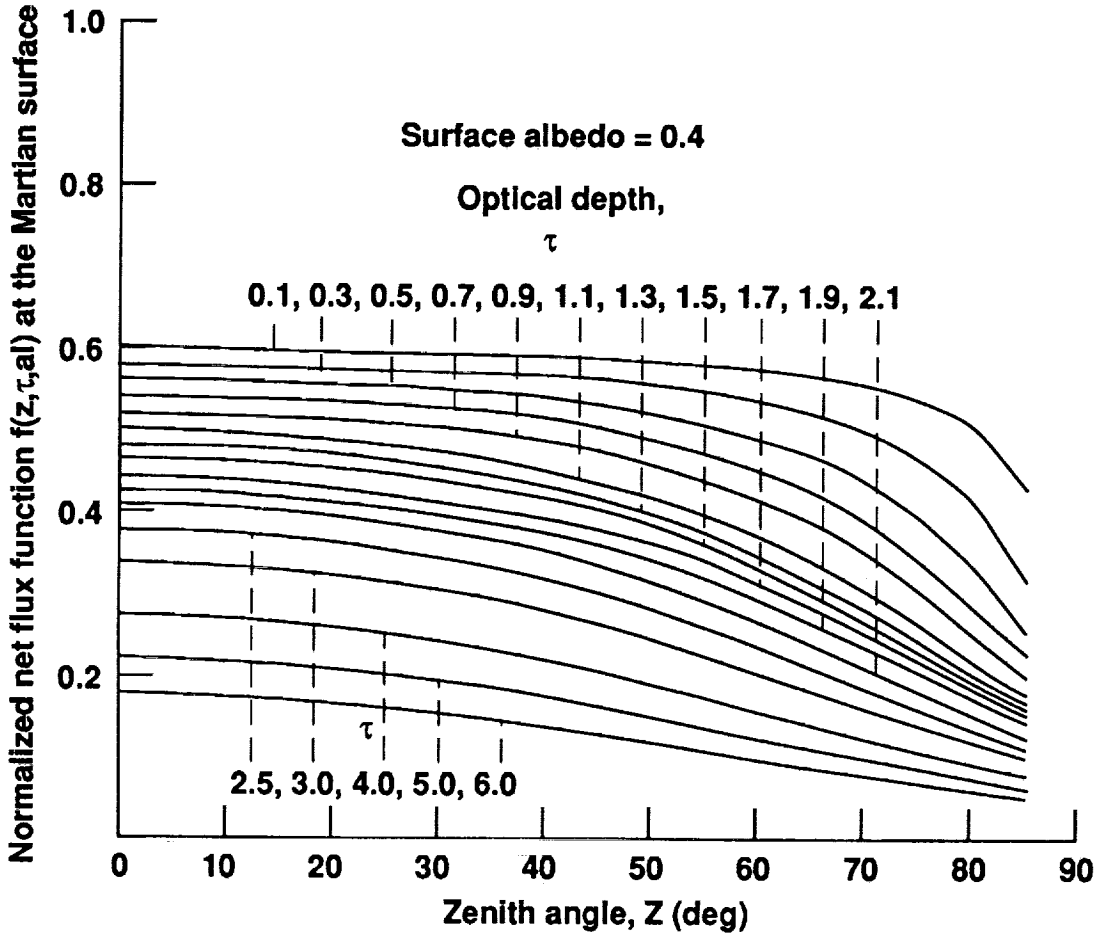

(b) Effect of Sun zenith angle with optical depth as a parameter

Fig. 9 - Concluded

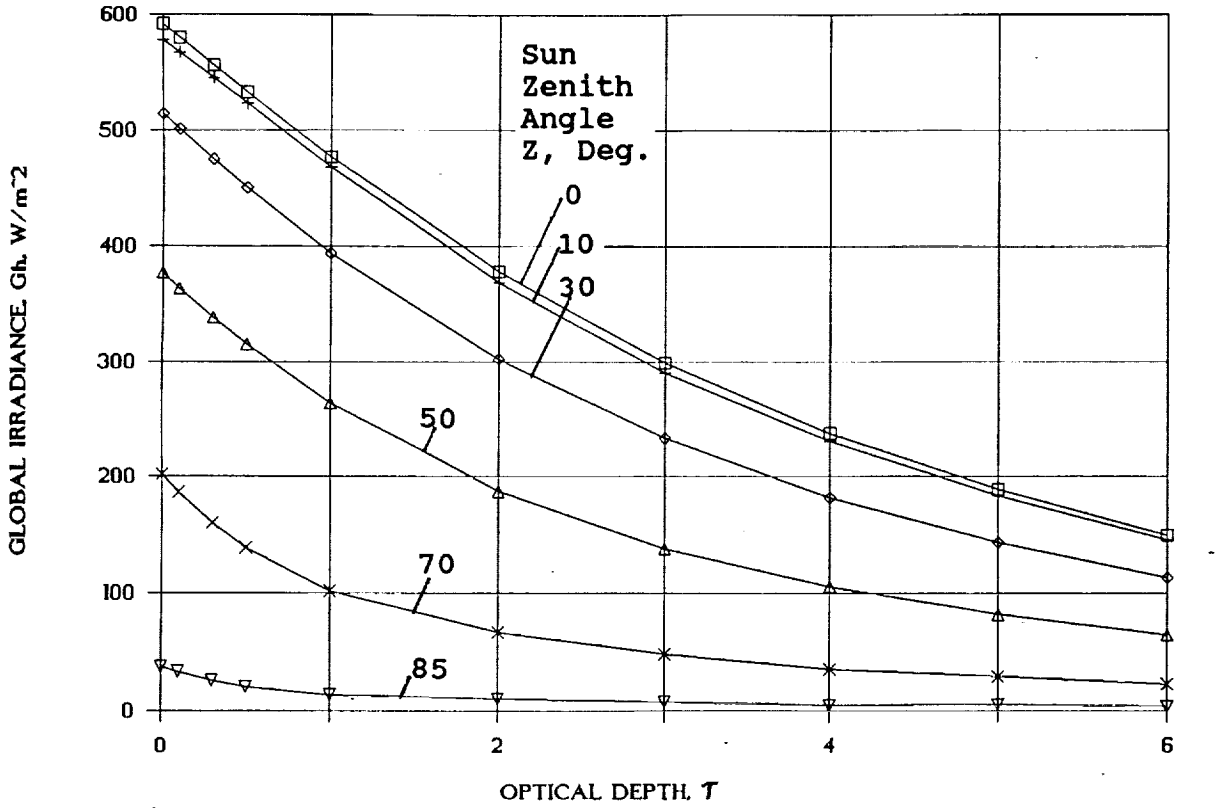

(a) Effect of optical depth with Sun zenith angle as a parameter

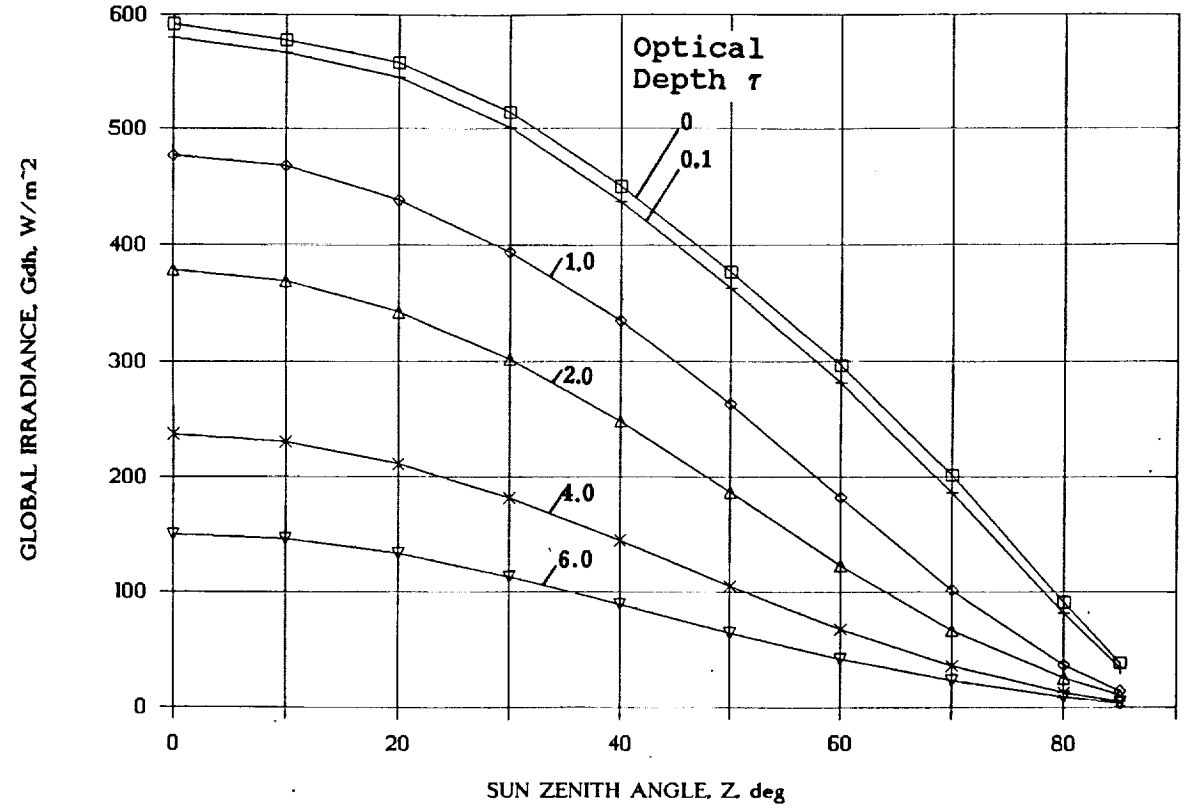

(b) Effect of Sun zenith angle with optical depth as a parameter

Fig. 10 - Variation of the global irradiance with optical depth and Sun zenith angle on a horizontal surface, at mean irradiance of 590 W/m^2

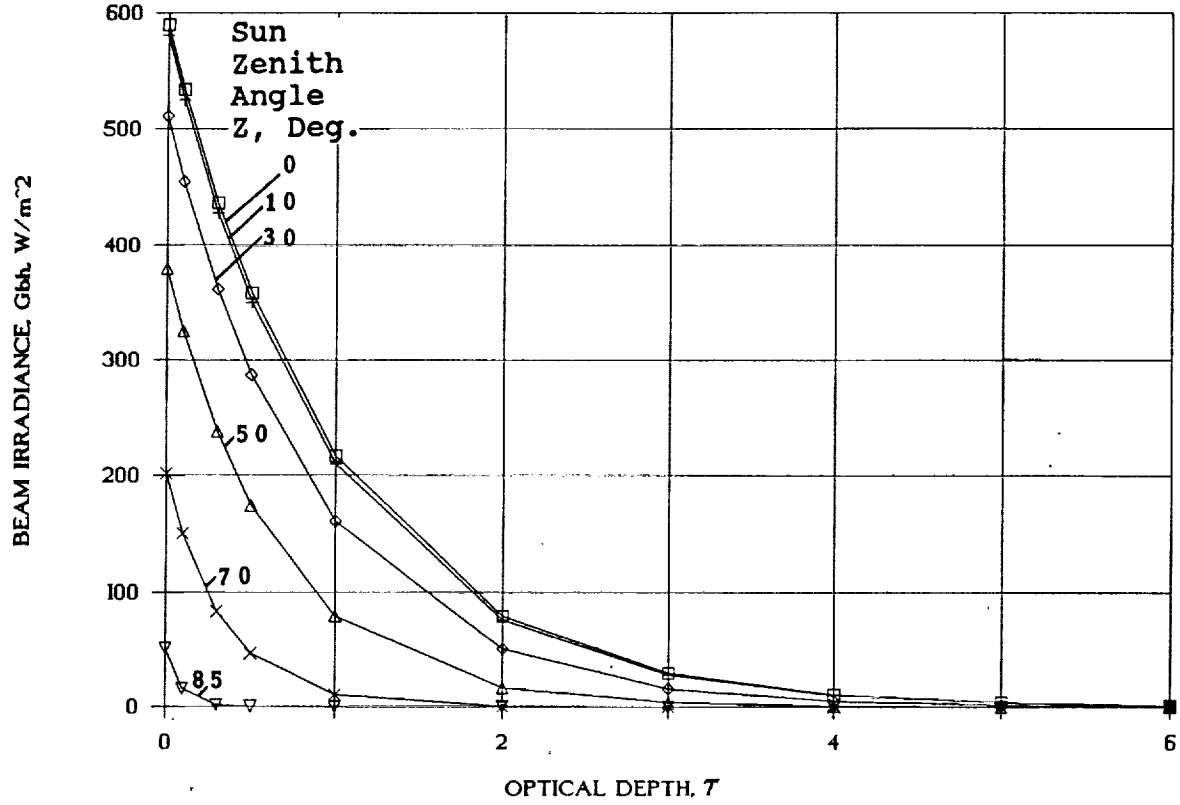

(a) Effect of optical depth with Sun zenith angle as a parameter

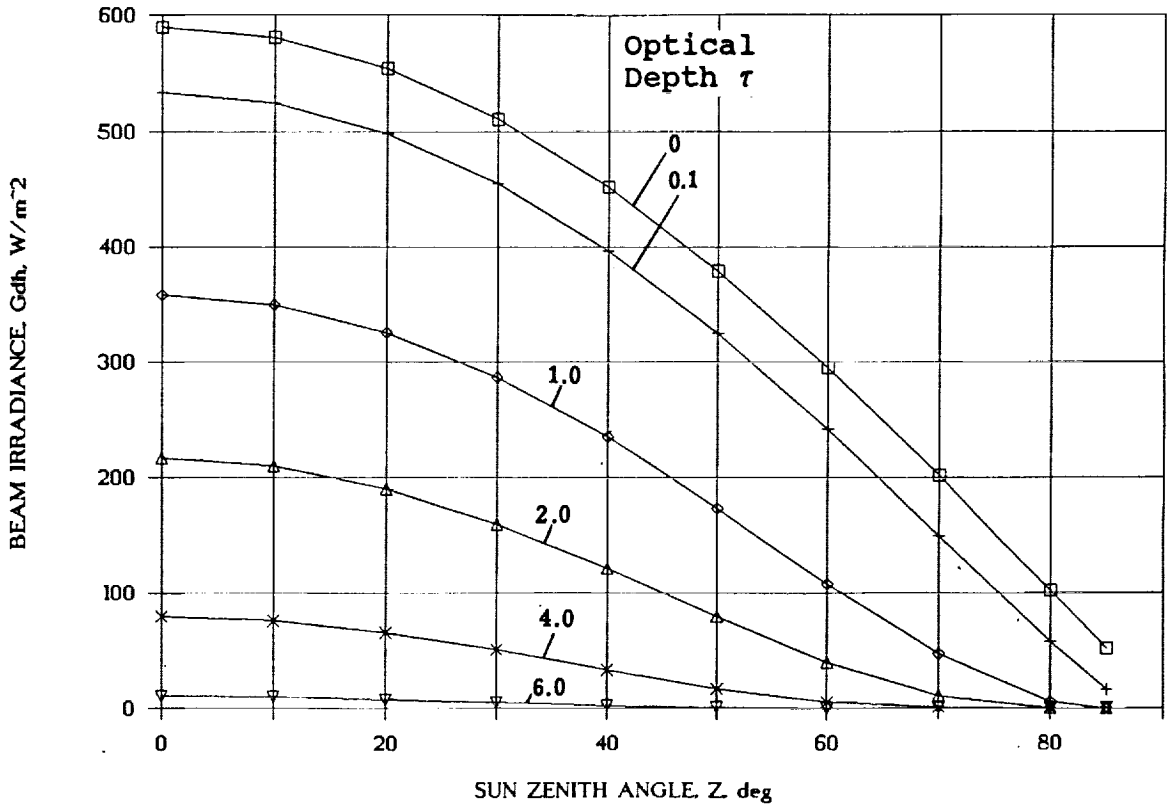

(b) Effect of Sun zenith angle with optical depth as a parameter

Fig. 11 - Variation of beam irradiance with optical depth and Sun zenith angle, on a horizontal surface, at mean irradiance of 590 W/m^2

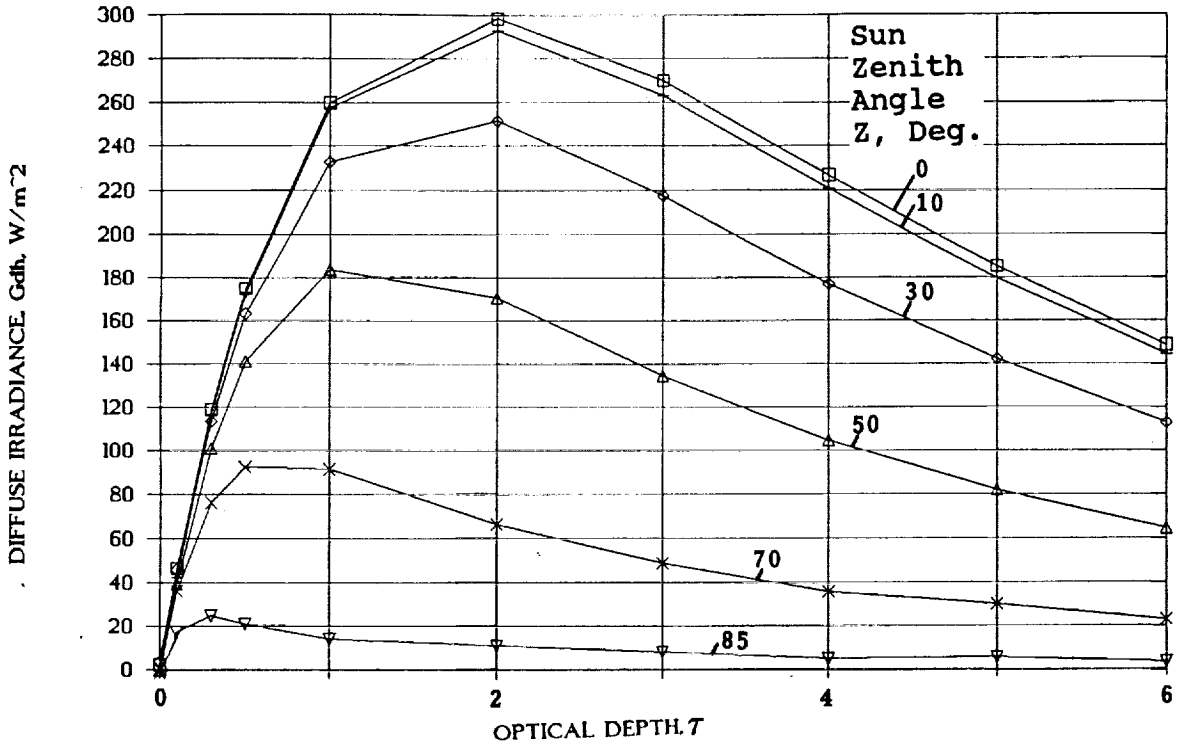

(a) Effect of optical depth with Sun zenith angle as a parameter

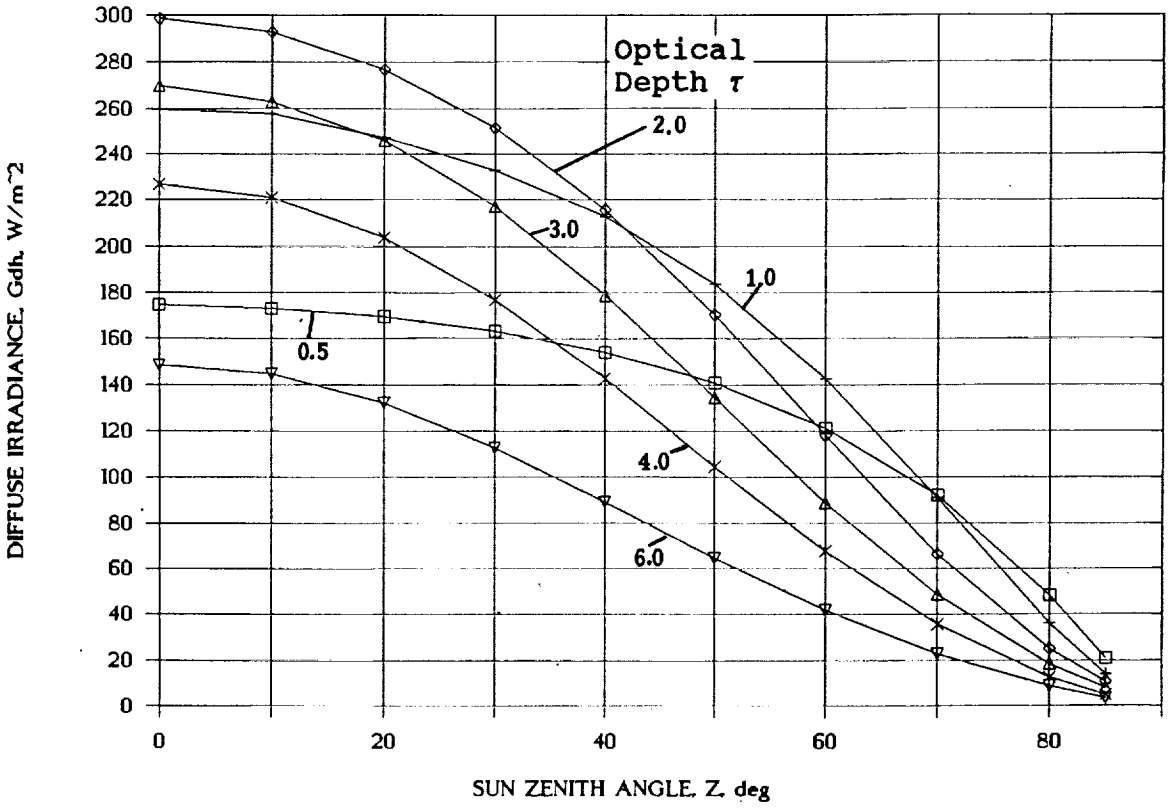

(b) Effect of Sun zenith angle with optical depth as a parameter

Fig. 12 - Variation of diffuse irradiance with optical depth and sun zenith angle, on a horizontal surface, at mean irradiance of 590 W/m^2

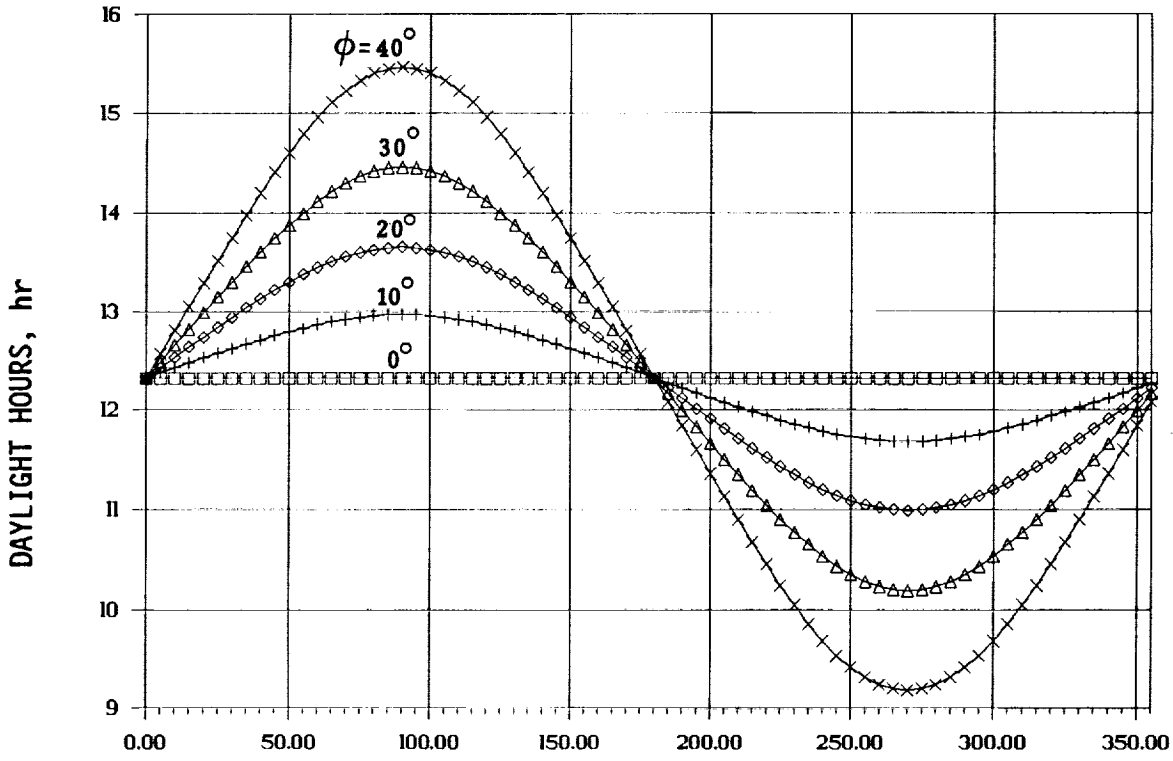

(a) Latitudes = 0°, 10°, 20°, 30°, 40°

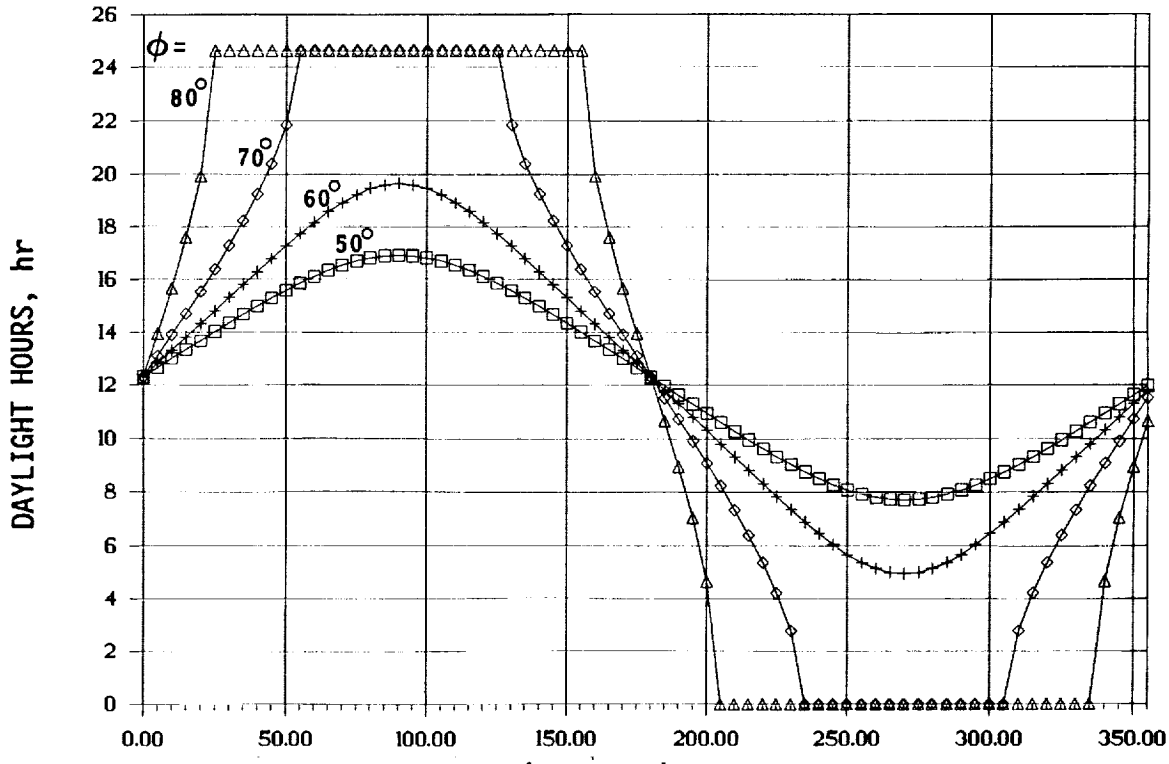

(b) Latitudes = 50°, 60°, 70°, 80°

Fig. 13 - Daylight hours (terrestrial), hr

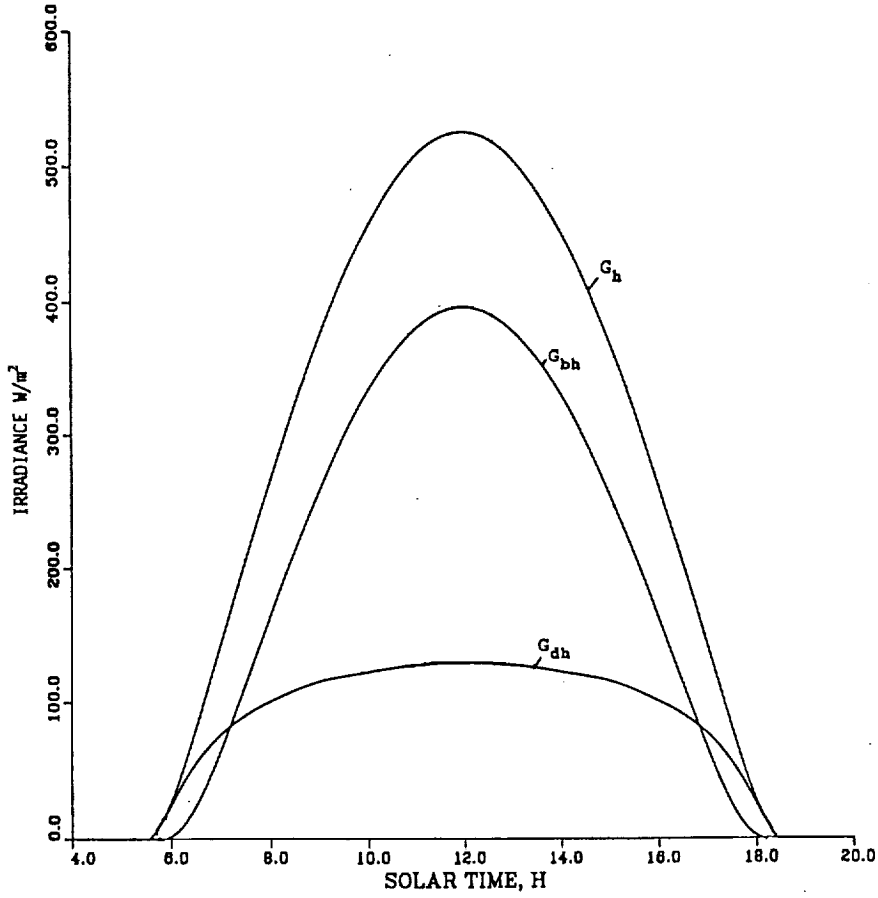

(a) For L_S = 141° and = 0.35 (lowest opacity)

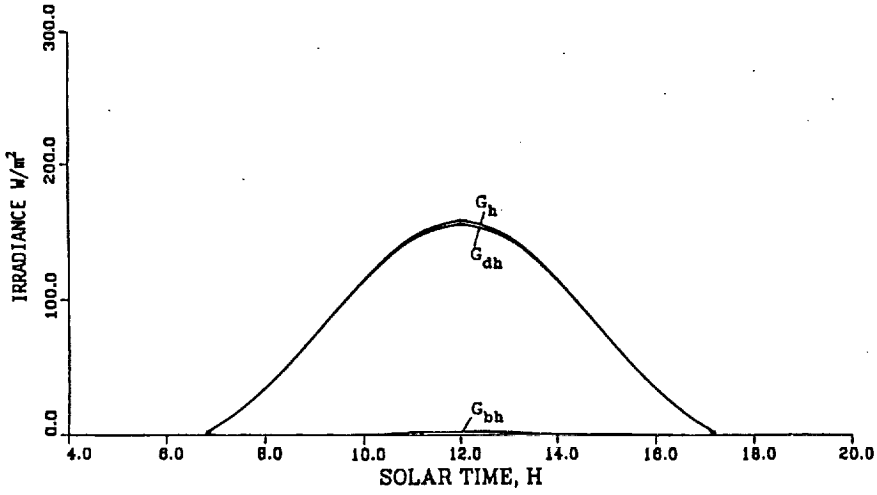

(b) For L_S = 291° and = 3.60 (highest opacity)

Fig. 14 - Diurnal variation of global G_h, beam G_{bh} and diffuse G_{dh} irradiance on a horizontal Mars surface at Viking Lander VL1

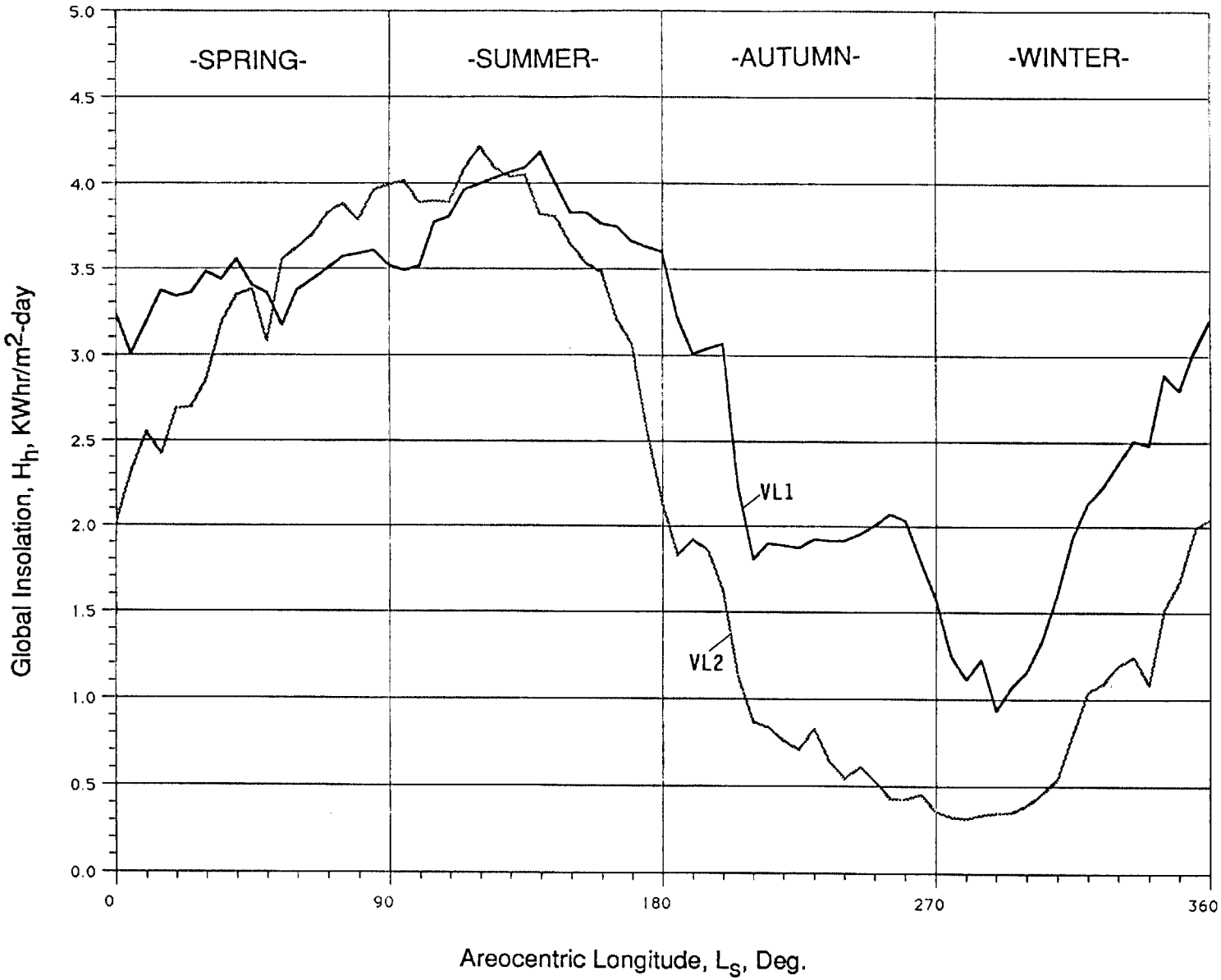

Fig. 15 - Daily global insolation on a horizontal surface on Mars for seventy two areocentric longitudes covering a Martian year, at VL1 and VL2

FIGURE 16a. - MARS MAP, 1:15,000,000, DEPARTMENT OF THE INTERIOR, U.S. GEOLOGICAL SURVEY.

FIGURE 16b. - MARS MAP, 1:15,000,000, DEPARTMENT OF THE INTERIOR, U.S. GEOLOGICAL SURVEY.

NASA
National Aeronautics and Space Administration

Report Documentation Page

1. Report No.	2. Government Accession No.	3. Recipient's Catalog No.
NASA TM-103623		

4. Title and Subtitle	5. Report Date
Solar Radiation on Mars—Update 1990	October 1990
	6. Performing Organization Code

7. Author(s)	8. Performing Organization Report No.
Joseph Appelbaum and Dennis J. Flood	E-5783
	10. Work Unit No. 506-41-11

9. Performing Organization Name and Address	11. Contract or Grant No.
National Aeronautics and Space Administration Lewis Research Center Cleveland, Ohio 44135-3191	
	13. Type of Report and Period Covered Technical Memorandum

12. Sponsoring Agency Name and Address	14. Sponsoring Agency Code
National Aeronautics and Space Administration Washington, D.C. 20546-0001	

15. Supplementary Notes

Joseph Appelbaum, National Research Council—NASA Research Associate and Tel Aviv University, Tel Aviv, Israel; work funded under NASA grant NAGW-2022. Dennis J. Flood, Lewis Research Center.

16. Abstract

Detailed information on solar radiation characteristics on Mars are necessary for effective design of future planned solar energy systems operating on the surface of Mars. In this paper we present a procedure and solar radiation related data from which the diurnally and daily variation of the global, direct beam and diffuse insolation on Mars are calculated. The radiation data are based on measured optical depth of the Martian atmosphere derived from images taken of the sun with a special diode on the Viking Lander cameras; and computation based on multiple wavelength and multiple scattering of the solar radiation. This work is an update to NASA TM 102299 and include a refinement of the solar radiation model.

17. Key Words (Suggested by Author(s))	18. Distribution Statement
Mars; Viking landers; Solar radiation; Irradiance; Insolation; Global, direct beam, and diffuse radiation; Optical depth; Local and global dust storms	Unclassified – Unlimited Subject Category 92

19. Security Classif. (of this report)	20. Security Classif. (of this page)	21. No. of pages	22. Price*
Unclassified	Unclassified	36	A03

NASA FORM 1626 OCT 86

*For sale by the National Technical Information Service, Springfield, Virginia 22161